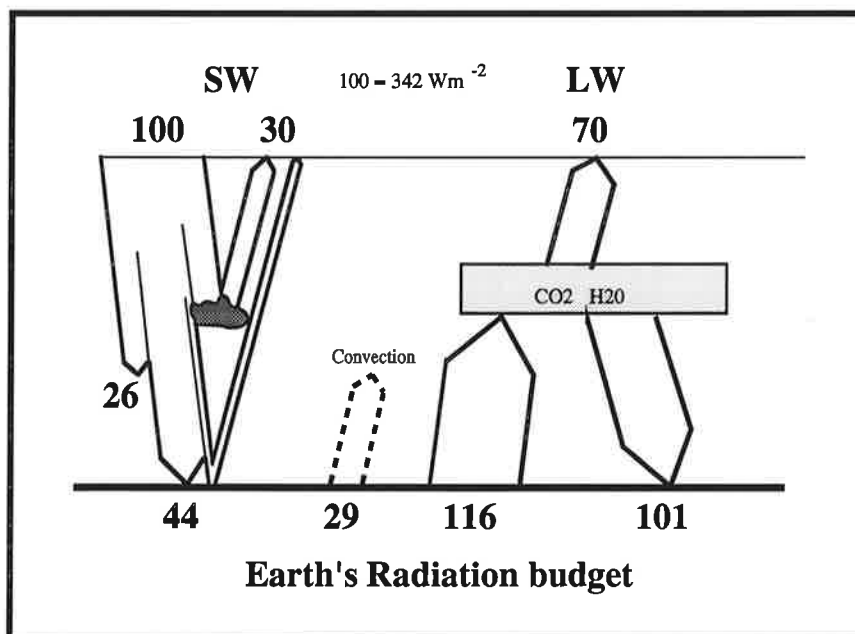




Max-Planck-Institut für Meteorologie

REPORT No. 200



IMPROVED REPRESENTATION OF SURFACE AND ATMOSPHERIC RADIATION BUDGETS IN THE ECHAM4 GENERAL CIRCULATION MODEL

by

Martin Wild • Atsumu Ohmura • Hans Gilgen • Erich Roeckner • Marco Giorgetta

HAMBURG, July 1996

AUTHORS:

Martin Wild,
Atsumu Ohmura,
Hans Gilgen:

Swiss Federal Institute of Technology
ETH, Zürich
Switzerland

Erich Roeckner,
Marco Giorgetta:

Max-Planck-Institute for Meteorology
Hamburg
F. R. Germany

MAX-PLANCK-INSTITUT
FÜR METEOROLOGIE
BUNDESSTRASSE 55
D-20146 HAMBURG
F.R. GERMANY

Tel.: +49 - (0)40 - 411 73 - 0
Telefax: +49 - (0)40 - 411 73 - 298
E-Mail: <name>@dkrz.de

ISSN 0937 – 1060

**Improved representation of surface and
atmospheric radiation budgets in the
ECHAM4 General Circulation Model**

Martin Wild, Atsumu Ohmura, Hans Gilgen

Swiss Federal Institute of Technology ETH, Zürich

Erich Roeckner, Marco Giorgetta

Max Planck Institute for Meteorology, Hamburg

ISSN 0937-1060

Abstract

The surface and atmospheric radiation budgets of the latest version of the Max-Planck Institute GCM, the ECHAM4, differ considerably from the earlier version ECHAM3 and other GCMs in both short- and longwave ranges. The absorbed shortwave radiation at the surface is substantially smaller (147 Wm^{-2}) than typically found in current GCMs, due to a larger atmospheric absorption of 90 Wm^{-2} . The enhanced shortwave atmospheric absorption is related to an increase of both simulated clear-sky and cloud absorption. Observational evidence is presented that this revised disposition of shortwave absorption is more realistic than typically found in current GCMs. This conclusion is based on a comparison of the model radiative fluxes with a large number of surface and collocated top-of-atmosphere observations, as well as stand-alone validations of the radiation scheme. In contrast to other GCMs which show a smaller atmospheric and a larger surface shortwave absorption, respectively, the ECHAM4 shortwave absorption is closer to the observations.

The clear-sky surface insolation of the ECHAM4 radiation scheme is shown to be very accurately calculated in a stand-alone validation, compared to other schemes which tend to overestimate these fluxes. This suggests that the global mean ECHAM4-calculated clear-sky shortwave absorption of 72 Wm^{-2} within the atmosphere and 214 Wm^{-2} at the surface are realistic values. Further, the ECHAM4-calculated cloud amount is in good agreement with surface-based observations. The above findings imply that the increase in the cloud absorption in ECHAM4 (TOA-to-surface cloud radiative forcing ratio R of 1.35) is consistent with the available observations on the global scale.

Zonally, observational evidence for a necessity to increase cloud absorption in GCMs is found in the low latitudes in agreement with other recent studies, but not so in the higher latitudes: the comparisons favour a value of R near 1.3 - 1.4 in the tropics but closer to 1 in the extratropics.

Overall, this study indicates that not only an increased solar absorption by clouds but also by the cloud-free atmosphere is essential to reduce the discrepancies between GCM-calculated atmospheric shortwave absorption and observations.

The smaller surface insolation and associated reduction of the available energy at the surface is partly compensated for by an increased downward longwave flux at the surface (344 Wm^{-2} in ECHAM4), which is considerably larger than in other GCMs. The larger downward longwave flux is supported by surface measurements and by a stand-alone validation of the radiation scheme for clear-sky conditions. The enhanced downward longwaveflux allows to maintain the level of available energy at the surface needed for a realistic intensity of the global hydrological cycle.

1 Introduction

The radiation budget of the earth is fundamental for the understanding of the genesis and evolution of the global climate system. Due to the recent advances of space-borne measurements, the net solar energy absorbed by the global climate system is accurately known (Barkstrom et al., 1990). However, it is not equally as well known how the energy absorption is partitioned between the atmosphere and the earth's surface. This uncertainty is reflected in the current generation of General Circulation Models (GCM), which show substantial differences in these fundamental quantities (Gutowski et al., 1991; Randall et al., 1992; Wild et al., 1995b).

Using a large number of surface observations, Wild et al. (1995b) concluded that current GCMs overestimate the absorption of solar radiation at the surface and ascribed it to an underestimation of solar absorption within the atmosphere. An underestimated atmospheric absorption can be due to either underestimated cloud or clear-sky absorption. Recently, evidence has been presented that the GCM-calculated absorption of solar radiation by clouds is underestimated (Cess et al., 1995; Ramanathan et al., 1995). Moreover, Li and Barker (1994) and Wild et al. (1995b) presented evidence that the GCM-calculated absorption of solar radiation in the cloud-free atmosphere is underestimated. Kiehl et al. (1995) demonstrated with the NCAR CCMII GCM, that an increased shortwave atmospheric absorption (due to increased cloud absorption in that case) can have a significant impact on the simulated model climate.

The overestimation of the absorbed solar radiation at the surface has been identified as a general problem in many state-of-the-art GCMs (Li and Barker, 1994; Garratt, 1994; Wild et al., 1995b). The global mean surface absorption of solar radiation is in most GCMs substantially higher than estimates based on surface observations (142 Wm^{-2} , Ohmura and Gilgen, 1992) and satellite observations (157 Wm^{-2} , Li and Leighton, 1993).

The latest version of the Max-Planck Institute (MPI) model series, ECHAM4, calculates considerably lower values of absorbed solar radiation at the surface than the earlier ECHAM3 version and other GCMs due to an enhanced absorption of solar radiation within the atmosphere. This enhancement is a result of both increased cloud and clear-sky absorption by almost equal amounts. In this study, a new dataset of direct observations is used for the assessment of the disposition of the GCM-calculated solar absorption within the climate system, and an attempt is made to estimate the relative importance of clear-sky and cloud absorption in the atmospheric radiation budget.

The longwave (thermal) radiation emitted to space by the climate system to balance the net solar absorption is also well established through satellite measurements (Barkstrom et al., 1990). The longwave exchange between the earth's surface and the atmosphere, however, is known with a much lesser confidence. Particularly, the downwelling atmospheric thermal emission towards the surface (downward or incoming longwave radiation) is only poorly known on the global scale. Accordingly, considerable differences exist in the simulated incoming longwave flux in different GCMs. Wild et al. (1995b) presented evidence that the incoming longwave radiation at the earth's surface is underestimated in ECHAM3 and other GCMs. Similar findings were reported in a recent study by Garratt and Prata (1996). Apart from the GCMs, a general trend for underestimation of the incoming longwave radiation by previous works in radiation climatology was speculated

by Ohmura and Gilgen (1992). The global mean ECHAM4 incoming longwave radiation at the surface is substantially larger than in ECHAM3 and other GCMs. Observational support for an increased flux of GCM-calculated incoming longwave radiation is given in this study.

In Section 2 the ECHAM3 and ECHAM4 models are described, which are analysed in detail in this study. The experiments performed with these models are presented in Section 3. Section 4 references the observational data sources. The GCM-simulated shortwave and longwave fluxes are analyzed in Section 5 and 6, respectively. Section 7 summarizes the principal findings of this study.

2 Models

The two GCMs analysed are the third and fourth generation versions of the ECHAM GCM, ECHAM3 and ECHAM4, respectively, developed at the Max Planck Institute for Meteorology, Hamburg. Additionally, global mean radiation budget values from a number of other GCMs have been collected from the literature and through personal communication.

The ECHAM3 GCM is described in detail in Roeckner et al. (1992). This GCM has evolved from the spectral numerical weather forecasting model of the European Centre for Medium Range Weather Forecasts (ECMWF) and has been extensively modified in Hamburg for climate applications. These modifications include an additional prognostic equation for cloud water (Roeckner et al., 1991), a new surface parameterization scheme (Dümenil and Todini, 1992) and the radiation scheme of Hense et al. (1982).

This radiation scheme is based on a two-stream approximation described by Kerschgens et al. (1978) and Zdunkowski et al. (1980) with delta-Eddington approximation for clouds. The longwave spectrum is divided into 6 spectral intervals taking into account absorption due to water vapor, carbon dioxide, ozone and aerosol. An inversion procedure is employed to define the relevant optical properties by matching the two-stream solutions to more accurate model solutions obtained by a line-by-line model (Hense et al., 1982), based on spectroscopic data of LOWTRAN3 (Selby and McClatchey, 1975). For cloud droplet absorption an emissivity formulation is used (Stephens, 1978). Scattering of longwave radiation is neglected. The shortwave spectrum is divided into four intervals ranging from $0.215 \mu\text{m}$ - $3.58 \mu\text{m}$, with the same gaseous absorbers as above (Table 1). The optical thickness for gas absorption is a function of the effective absorber amount and is determined similarly to the longwave part. Rayleigh scattering is included via a parametric expression of optical thickness. Scattering and absorption coefficients of stratospheric, urban, and maritime aerosols are taken from a dataset provided by Shettle and Fenn (1976). Cloud optical depth and single scattering albedo are derived from the cloud water path (Stephens, 1978).

The ECHAM4 incorporates the most recent improvements in a number of key climatic processes, described in Roeckner et al. (1996). One of the most fundamental changes between the ECHAM3 and the ECHAM4 model is the inclusion of a completely new radiation code. This code is based on the scheme developed by J.J. Morcrette for the numerical weather prediction model, cycle 43, of the ECMWF (Morcrette, 1991).

Table 1: Spectral intervals and absorber in the solar part of the ECHAM3 (Hense et al. 1982) and ECHAM4 (Morcrette 1991) radiation schemes.

Model	Spectral Interval (μm)	Absorber
ECHAM3	0.215-0.685	O3
	0.685-0.891	H2O
	0.891-1.273	H2O
	1.273-3.580	H2O, CO2
ECHAM4	0.25-0.68	O3
	0.68-4.0	H2O, CO2

This scheme uses a two-stream method based on Fouquart and Bonnel (1980) for the solar part and Morcrette et al. (1986) for the longwave part. The solar spectrum is divided only into two bands (Table 1). Coefficients for the gaseous absorption are calculated from the 1982 version of the Air Force Geophysics Laboratory (AFGL) line parameters compilation (Rothman et al., 1983). Rayleigh scattering is included via a parametric expression of optical thickness. Aerosol scattering and absorption coefficients are based on Shettle and Fenn (1976) as in ECHAM3. The cloud shortwave radiative properties are a function not only of the cloud water path as in ECHAM3, but also of the effective radius of the cloud particles. The longwave spectrum is divided into six bands with gas absorption coefficients fitted from AFGL 1982. The water vapour continuum parameterization is based on Roberts et al. (1976). As in ECHAM3, clouds are treated as grey bodies with a longwave emissivity depending on the cloud water path (Stephens, 1978).

The ECMWF code has undergone a number of changes at MPI. Additional greenhouse gases such as methane, nitrous oxide, 16 CFCs, and the 14.6 μm band of ozone have been considered as well as various types of aerosols (R. v. Dorland, personal communication 1995). Moreover, the water vapor continuum has been revised to include temperature weighted band averages of e-type absorption and also a band dependent ratio of (p-e)-type to e-type continuum absorption (Giorgetta and Wild, 1995). The single scattering properties of cloud droplets and ice crystals are determined on the basis of high-resolution Mie calculations with subsequent averaging over the relatively wide spectral range of the GCM with appropriate weighting by the Planck function (Rockel et al., 1991). This procedure has been applied for different effective radii, and polynomial fits are finally employed which allow to express the single scattering parameters as analytical functions of the effective radius within the respective spectral domain. Since the effective radii are parameterized in terms of the simulated liquid and ice water content, respectively, the cloud optical properties are basically determined by the model itself (Roeckner, 1995).

3 Experiments

The analysis of the radiative fluxes is based on simulations performed with ECHAM3 and ECHAM4 using present day boundary conditions ("control runs"). In these experiments, sea surface temperatures and sea ice were prescribed daily by linear interpolation between mean monthly climatologies from the AMIP SST and sea-ice dataset (Gates, 1992).

The simulations have been performed with different model horizontal resolutions up to wavenumber T106 (1.1° gridspacing). The ECHAM3 and ECHAM4 high resolution (T106) simulations were integrated for 5 and 10 years, respectively, at the Swiss Scientific Computing Center (CSCS), in a joint project of the Max Planck Institute for Meteorology, Hamburg, and the Swiss Federal Institute of Technology, Zurich. Multidecadal integrations at lower resolution (T21, T42) using the same experiment type have been performed at the Max Planck Institute with both models.

Wild et al. (1995b) showed that the horizontal resolution has no significant effect on the global and zonal mean simulation of the surface radiative budgets in ECHAM3 simulations ranging from T21 to T106. The surface, atmospheric and top-of-atmosphere budgets of ECHAM3 and ECHAM4 were also found to vary insignificantly with horizontal resolution on the global and zonal scale. The results shown below are generally based on the T42 simulations, since additional clear-sky diagnostics were available for both model versions at this resolution. However, the conclusions presented in this study do not critically depend on the horizontal resolution of the models.

4 Observational data

This study is entirely based on directly measured radiative fluxes. Semi-empirical estimates are not used. The surface flux climatologies are retrieved from a database for the instrumentally measured surface energy fluxes, the Global Energy Balance Archive (GEBA, Ohmura et al., 1989; Gilgen et al., 1996). This database currently possesses 220'000 monthly mean fluxes for about 1600 sites and has been used in a number of studies to assess GCM and satellite derived estimates of surface energy fluxes (e.g., Garratt, 1994; Li et al., 1995; Wild et al., 1995b; Wild et al., 1995a; Wild et al., 1996; Rossow and Zhang, 1995; Garratt and Prata, 1996). The measurement uncertainty for the incoming shortwave radiation values in GEBA is estimated to be within 2%, while 5% for the incoming longwave radiation.

The satellite climatologies of the radiative fluxes at the top-of-atmosphere (TOA) which are collocated with the observation stations at the surface are ensemble averages from the Earth Radiation Budget Experiment (ERBE, Barkstrom, 1984) over the period 1985 - 1989, with a resolution of 2.5°x 2.5°. The uncertainties in the monthly averaged scanner data are estimated at +/- 5 Wm⁻² (Barkstrom et al., 1990).

For the assessment of the radiation scheme in stand-alone mode, selected surface radiation measurements of high quality and high temporal resolution are used together with upper air soundings from the aerological station of Payerne in Switzerland. Payerne is one of the ten presently active stations in the Baseline Surface Radiation Network (BSRN) of the World Climate Research Program (WCRP, 1991).

5 Shortwave radiation

The global mean absorbed shortwave radiation at the earth's surface calculated by ECHAM3, ECHAM4 and a number of other GCMs from the literature and personal communications is displayed in Fig. 1. Large differences in the range of almost 40 Wm^{-2} in the global mean are found among the GCMs.

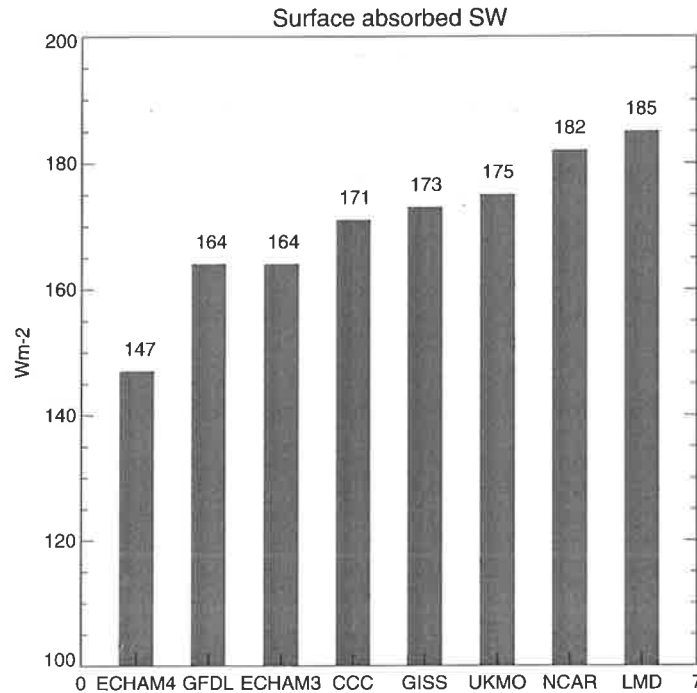


Figure 1: Global annual mean absorbed shortwave radiation at the surface of the ECHAM3, ECHAM4 and other GCMs. NCAR, GFDL, GISS values from Gutowski et al. (1991), CCC value from Boer (1993), LMD value from J. Polcher (pers. communication, based on model version LMD6). UKMO value from H. Cattle (pers. communication). Units Wm^{-2} .

The ECHAM4 value, at 147 Wm^{-2} , is substantially smaller than the value of the earlier ECHAM3 version and other GCMs.

Wild et al. (1995b) demonstrated that the incoming shortwave radiation at the surface in the ECHAM3 GCM is substantially overestimated compared to a comprehensive dataset of surface observations. Based on considerations of global mean values it was suggested that the overestimation of the surface fluxes is due to a too transparent atmosphere (Wild et al., 1995b). This argument is further expanded here using additionally collocated satellite observations of the top-of-atmosphere (TOA) radiative fluxes above the sites where surface observations are available. Combining the flux measurements at the surface and at the TOA allows a direct estimate of the shortwave atmospheric absorption.

For this purpose, the gridded model and ERBE data are interpolated to the 720 GEBA sites that were used in Wild et al. (1995b), taking into account the four surrounding gridpoints weighted by their inverse spherical distance. The global distribution of the GEBA sites is shown in Figure 1 of Wild et al. (1995b).

To determine the accuracy of the total absorbed solar energy in the surface-atmosphere system at the 720 GEBA locations, differences between the annual mean ECHAM3-calculated net shortwave fluxes at the TOA and the ERBE fluxes are shown in Fig. 2a. The agreement is within 20 Wm^{-2} at most of the sites. Globally, the model-calculated total absorbed shortwave energy of 235 Wm^{-2} is within the measurement uncertainty of the ERBE value of 237 Wm^{-2} (Barkstrom et al., 1990). This good agreement of the global mean values is partly the result of a tuning in the cloud scheme to match the global mean planetary albedo with the satellite estimate. The global mean surface and TOA radiation budgets of ECHAM3 and ECHAM4 are summarized in Table 2.

Table 2: Global mean values of surface, atmospheric and top of atmosphere radiation budgets in ECHAM3 and ECHAM4. Units Wm^{-2} .

		ECHAM3 Wm^{-2}	ECHAM4 Wm^{-2}
Top of Atmosphere	SW absorbed all-sky	235	237
	SW absorbed clear-sky	284	286
	SW cloud radiative forcing	-49	-49
	LW emitted all-sky	-233	-235
	LW emitted clear-sky	-262	-263
	LW cloud radiative forcing	29	28
Atmosphere	SW absorbed all-sky	71	90
	SW absorbed clear-sky	63	72
	SW cloud radiative forcing	8	18
Surface	SW incoming all-sky	189	170
	SW absorbed all-sky	164	147
	SW absorbed clear-sky	222	214
	SW cloud radiative forcing	-58	-67
	LW incoming all-sky	334	344
	LW incoming clear-sky	311	323
	LW upward	397	397
	Net LW all-sky	-63	-53
	LW cloud radiative forcing	-23	-21
	Net radiation all-sky	101	95

The ECHAM3-calculated incoming shortwave radiation at the surface has been compared with the GEBA sites in Wild et al. (1995b). The absorbed shortwave radiation at the surface, however, is measured only at a few sites. To obtain a reference dataset for the absorbed shortwave radiation rather than the incoming shortwave radiation at the surface, the observed values of the incoming shortwave radiation have been combined with the collocated values of the surface albedo climatology used in ECHAM3 (Geleyn and Preuss, 1983). Differences between this dataset and the ECHAM3-calculated surface shortwave absorption at the GEBA sites are shown in Fig. 2c. These differences show the errors in the ECHAM3-calculated shortwave surface absorption induced by shortcomings in the simulated incoming shortwave radiation. Possible errors due to deficiencies in the model surface albedo are thereby neglected. The likely range of the albedo error, however, cannot

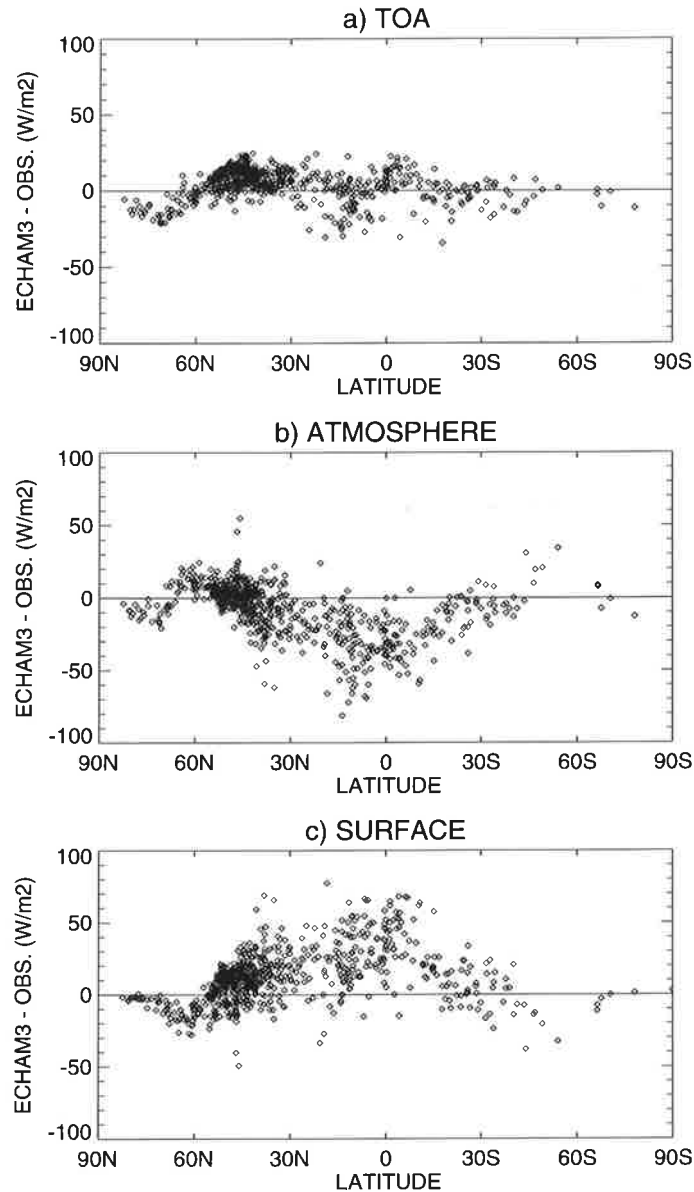


Figure 2:

a) Difference between *ECHAM3*-calculated and observed annual net shortwave fluxes at the top-of-atmosphere above 720 GEBA sites as a function of the sites' latitudes. Observations from *ERBE*.

b) Differences in *ECHAM3*-calculated and observed annual atmospheric shortwave absorption at the GEBA sites derived from differences in net TOA and surface fluxes as a function of the sites' latitudes.

c) Difference between *ECHAM3*-calculated and observed annual net shortwave fluxes at the surface as a function of the sites' latitudes. Observations from *GEBA*. Units Wm^{-2} .

explain the large magnitude of the differences in Fig. 2c. Replacing the Geleyn and Preuss (1983) surface albedo climatology by a more recently established climatology (Claussen et al., 1994) showed no significant impact on the calculated differences. These differences suggest a substantial model-overestimation of the absorbed shortwave radiation in the low latitudes and a slight underestimation at higher latitudes, as noted in Wild et al. (1995b) for the incoming shortwave radiation at the surface.

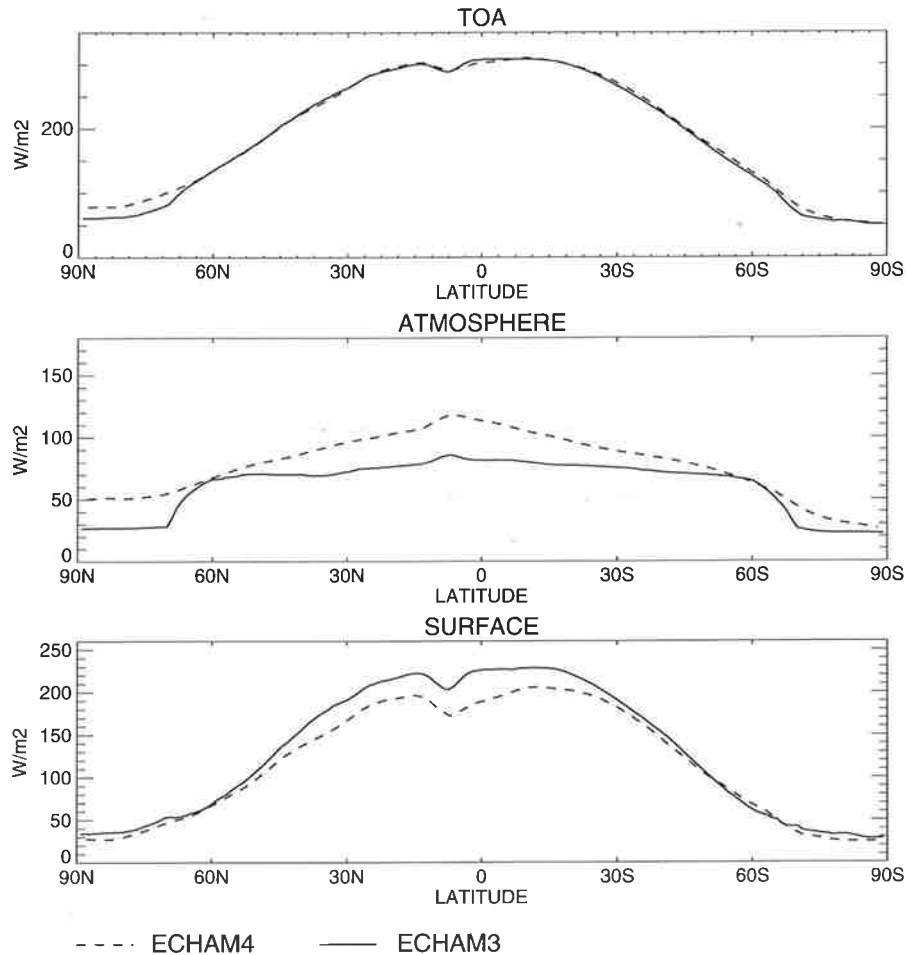


Figure 3: Zonal mean shortwave absorption in the ECHAM3 and ECHAM4 GCMs at the top-of-atmosphere (TOA), within the atmosphere and at the surface. Units Wm^{-2} .

Differences in the atmospheric absorption are determined as residuals of the net flux differences at the top of atmosphere and at the surface (Fig. 2b). Fig. 2b strongly suggests that the differences in the ECHAM3-calculated and observed fluxes found at the surface are predominantly due to differences in the atmospheric absorption rather than due to differences in the net solar fluxes at the TOA. Thus, the problem of the GCM-simulated radiative budget is not so much to capture the correct total amount of solar energy absorbed by the climate system but rather the partitioning of the energy absorbed in the atmosphere and at the surface.

Fig. 2b further indicates that the ECHAM3 shortwave atmospheric absorption is underestimated on the global scale, taking into account the fact that half of the earth's surface is located between 30°N and 30°S , where the underestimation is largest. This suggests that the global mean shortwave atmospheric absorption of 71 Wm^{-2} calculated in ECHAM3 must be a substantial underestimation.

These results are in line with the findings of Li and Barker (1994) of an underestimated atmospheric absorption in the Canadian Climate Center model CCCII and in the National Center for Atmospheric Research model CCM2, which at 58 and 67 Wm^{-2} , respectively, is even lower than in ECHAM3. This further confirms that the underestimation of atmospheric absorption of solar radiation is a common problem of many current GCMs.

As can be seen from Table 2, the latest model version of ECHAM, the ECHAM4 calculates a substantially larger atmospheric absorption (90 Wm^{-2}) than the abovementioned models. A zonal comparison of the ECHAM3 and ECHAM4 shortwave radiation budgets at the top-of-atmosphere (TOA), in the atmosphere and at the surface is given in Fig. 3. While the TOA radiation budget, i.e. the net solar energy absorbed by the climate system, is very similar in ECHAM3 and ECHAM4, the partitioning of the solar absorption between the surface and atmosphere substantially differ in the ECHAM3 and ECHAM4 simulations. The ECHAM4 radiation budgets are assessed in the following using the methodology outlined above.

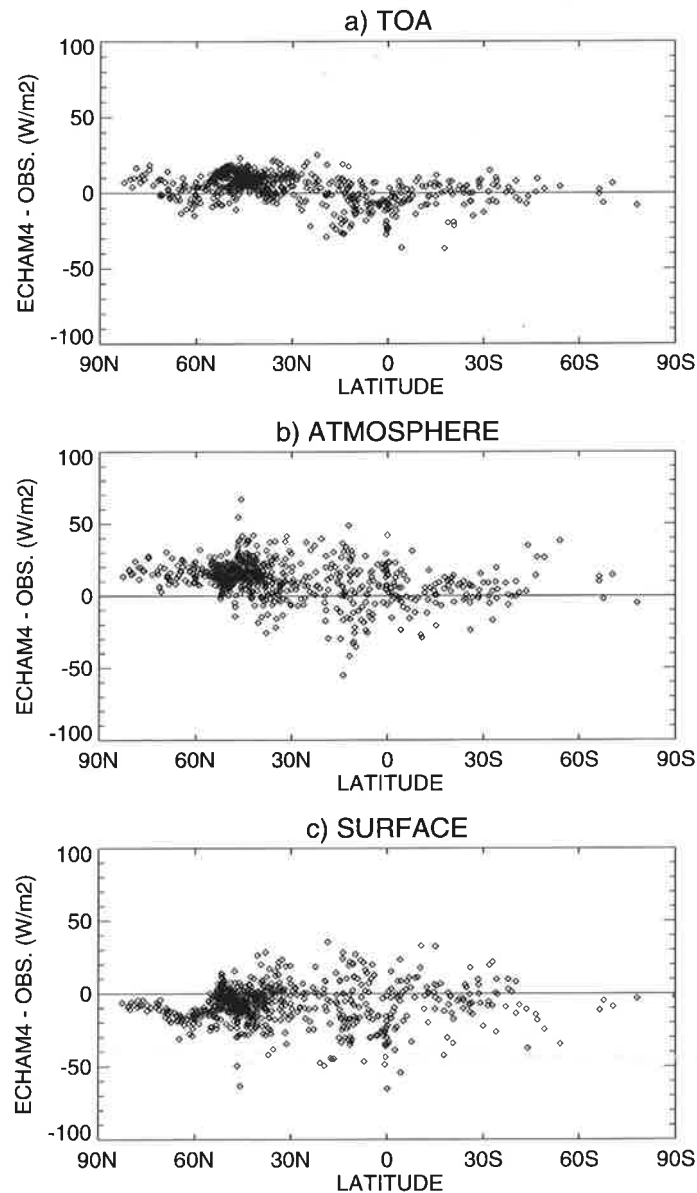


Figure 4: As Figure 2, but for ECHAM4.

Differences between the annual mean ECHAM4-calculated net shortwave fluxes at the TOA and the ERBE fluxes have been determined in Fig. 4a for the 720 locations. The differences are of similar magnitude as in ECHAM3 (Fig. 2a), with errors less than 20 Wm^{-2} . This is in line with Table 2 and Fig. 3, which showed that net shortwave fluxes at

the TOA in ECHAM3 and ECHAM4 do not differ greatly in the global and zonal mean. Also, global mean values of shortwave cloud radiative forcing and associated shortwave all-sky and clear-sky fluxes at the TOA do not change significantly in ECHAM4 (cf. Table 2) and are close to the respective values obtained in the ERBE experiment (Barkstrom et al., 1990). For a detailed discussion of the ECHAM4 TOA radiation budget the reader is referred to Chen and Roeckner (1996).

The ECHAM4-calculated absorbed shortwave radiation at the surface is compared with the 720 GEBA locations in Fig. 4c. As in the ECHAM3 comparison, the observed values of the incoming shortwave radiation have been combined with the collocated values of the surface albedo climatology used in the GCM to estimate the absorbed solar radiation at the ground. Compared to ECHAM3, the ECHAM4-calculated absorption of solar radiation at the surface has been substantially improved (cf. Figs. 2c and 4c). Particularly, the large overestimate on the order of 40 Wm^{-2} in ECHAM3 in the low latitudes is no longer present in ECHAM4. Rather, a slight tendency for underestimation is found. The too strong meridional insolation gradient found in ECHAM3 in the mid-latitudes is largely reduced. On the regional scale, a significantly improved simulation of the annual cycle of surface insolation in ECHAM4 was noted in Wild et al. (1996) for the specific region of Europe.

Fig. 4c shows that there is a tendency in ECHAM4 to underestimate the surface absorption in high latitudes. However, 77% of the earth's surface is located between 50°N and 50°S , where the surface absorption is in good agreement with observations in ECHAM4 but substantially overestimated in ECHAM3. This suggests that the 147 Wm^{-2} calculated global mean surface absorption in ECHAM4 is closer to reality than the 164 Wm^{-2} calculated by ECHAM3 or the values from other GCMs given in Fig. 1.

Considering that the surface absorption calculated with ECHAM4 shows a slight tendency of underestimation rather than overestimation in Fig. 4c suggests that the 147 Wm^{-2} sets a lower limit to the range of possible values of surface shortwave absorption. The mean bias between the model and observed surface absorption at the 720 sites, zonally weighted, is -5 Wm^{-2} for ECHAM4, while $+12 \text{ Wm}^{-2}$ in ECHAM3. This favours a most realistic value of global mean shortwave surface absorption slightly above 150 Wm^{-2} . This value is consistent with a recent estimate of global mean incoming shortwave radiation presented in Gilgen et al. (1996).

In Fig. 4b differences between the atmospheric absorption calculated with ECHAM4 and derived from observations are displayed. Compared to the ECHAM3 atmospheric shortwave absorption (Fig. 2b), the ECHAM4 atmospheric absorption is in better agreement with the observations, particularly the substantial underestimation of atmospheric absorption at low latitudes is completely removed. Rather, a tendency towards an overestimated atmospheric absorption is found in ECHAM4, particularly at higher latitudes, which is responsible for the slightly underestimated absorption at the surface. The overall overestimation of shortwave atmospheric absorption in ECHAM4 is, however, much smaller than its underestimation in ECHAM3. This suggests that the 90 Wm^{-2} global mean atmospheric absorption of ECHAM4 is closer to reality than the 71 Wm^{-2} of ECHAM3 given in Table 2. This supports recent observation-based estimates, which indicate a markedly higher atmospheric absorption of 98 Wm^{-2} (Ohmura and Gilgen, 1992) and 83 Wm^{-2} (Li and Leighton, 1993). The above comparisons may favour a global mean atmospheric

shortwave absorption near 85 Wm^{-2} as most realistic value.

Figs. 2 and 4 have shown that the improvements in the calculated surface fluxes in ECHAM4 compared to ECHAM3 are predominantly the result of an improved atmospheric absorption rather than changes in the planetary albedo and associated net shortwave fluxes at the TOA. As can be inferred from Table 2, the increased atmospheric absorption in ECHAM4 is due to both increased clear-sky and cloud absorption of almost equal amounts: 9 Wm^{-2} of the 19 Wm^{-2} enhanced atmospheric absorption in ECHAM4 are due to an increased clear-sky absorption of shortwave radiation (ECHAM3 63 Wm^{-2} , ECHAM4 72 Wm^{-2}), while the remainder of the 19 Wm^{-2} difference results from the enhanced absorption of the ECHAM4 clouds.

To assess whether the improved atmospheric absorption is due to both increased clear-sky and cloud absorption as suggested by ECHAM4, the clear-sky performance of the radiation scheme and the simulation of clouds are evaluated separately in the following.

5.1 Clear-sky

As noted above, the ECHAM4-calculated clear-sky atmospheric absorption is increased by 9 Wm^{-2} compared to ECHAM3 (Table 2).

The GCM-calculated radiative transfer in the cloud-free atmosphere depends on the formulation of the radiation scheme and on the distribution of absorbers and scattering particles in the atmosphere.

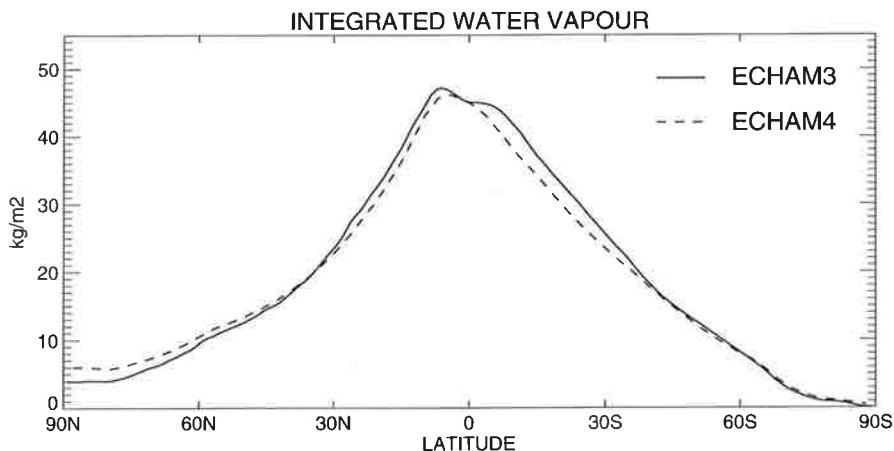


Figure 5: Vertically integrated atmospheric water vapour (annual mean), calculated with ECHAM3 and ECHAM4. Units kgm^{-2} .

Water vapour is the principal absorber of solar radiation in the cloud-free atmosphere. Both ECHAM4 and ECHAM3 generally agree with the satellite-observed abundance of water vapour (Chen et al., 1996). No major differences exist in the vertically integrated water vapour content of the ECHAM3 and ECHAM4 atmospheres on the global and zonal scale, as shown in Fig. 5. Thus, atmospheric water vapour cannot explain the differences between the radiative fluxes in the two model versions.

The prescribed distribution and radiative properties of the aerosols have not been changed from ECHAM3 to ECHAM4 and can neither explain the differences in the fluxes, as shown below. Thus, the different radiation schemes in ECHAM3 and ECHAM4 rather than differences in the atmospheric composition are considered as principal cause for the altered absorption in the cloud-free atmosphere.

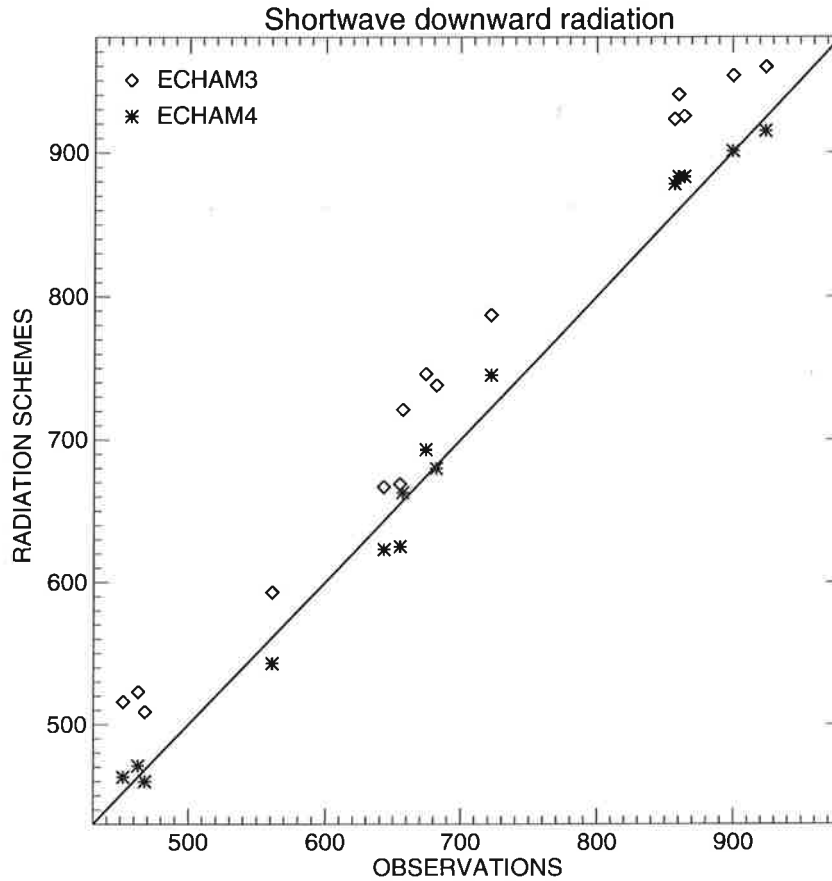


Figure 6: Incoming shortwave radiation at the surface under clear-sky conditions at noon: Stand-alone calculations with the ECHAM3 and ECHAM4 radiation schemes with prescribed atmospheric temperature and humidity profiles from radiosonde launches versus synchronous surface radiation measurements. Radiosonde data and radiation measurements from Payerne, Switzerland. Units Wm^{-2} .

Therefore, the clear-sky performance of the isolated ECHAM3 and ECHAM4 radiation schemes is assessed in a stand-alone mode. This is done using prescribed atmospheric profiles of temperature and humidity from radiosonde data as input to the radiation scheme, which allows a representative comparison of the model-calculated surface fluxes with in-situ measurements. This procedure was applied in Wild et al. (1995b) to the ECHAM3 radiation scheme and revealed a substantial overestimation of the clear-sky insolation at the surface. Here the same procedure is applied to the ECHAM4 radiation scheme. The observational data (radiosonde profiles, surface radiation measurements) stem from the Swiss aerological station in Payerne. The results of the stand-alone calculations with the ECHAM3 and ECHAM4 radiation schemes and the respective surface observations for a number of clear-sky situations are compared in Fig. 6. The calculations and measurements have been performed at noon local time, thus representing daily maximum values.

Fig. 6 shows that the ECHAM4-calculated fluxes agree substantially better with observations than the ECHAM3 fluxes and no longer overestimate the clear-sky irradiance. The mean over the cases in Fig. 6 is 700 Wm^{-2} for ECHAM3, 650 Wm^{-2} for ECHAM4 and 647 Wm^{-2} for the observed fluxes. Thus, the ECHAM4 radiation scheme is very close to the observations (within the measurement uncertainty, which is estimated at 2% for single measurements), while ECHAM3 substantially overestimates the surface fluxes by 50 Wm^{-2} . Note that these values are differences under daily maximum insolation at noon and should not be misunderstood as mean climatological differences which are much smaller. Integrated over the whole diurnal cycle these differences reduce to approx. 10 Wm^{-2} . These results of the one-dimensional radiation calculations are consistent with the 9 Wm^{-2} difference in the shortwave clear-sky surface and atmospheric budgets of the ECHAM4 and ECHAM3 three dimensional control runs (cf. Table 2). This confirms that the differences between the shortwave clear-sky radiation budgets of the two models are predominantly caused by the radiation schemes rather than by differences in the properties of the model atmospheres.

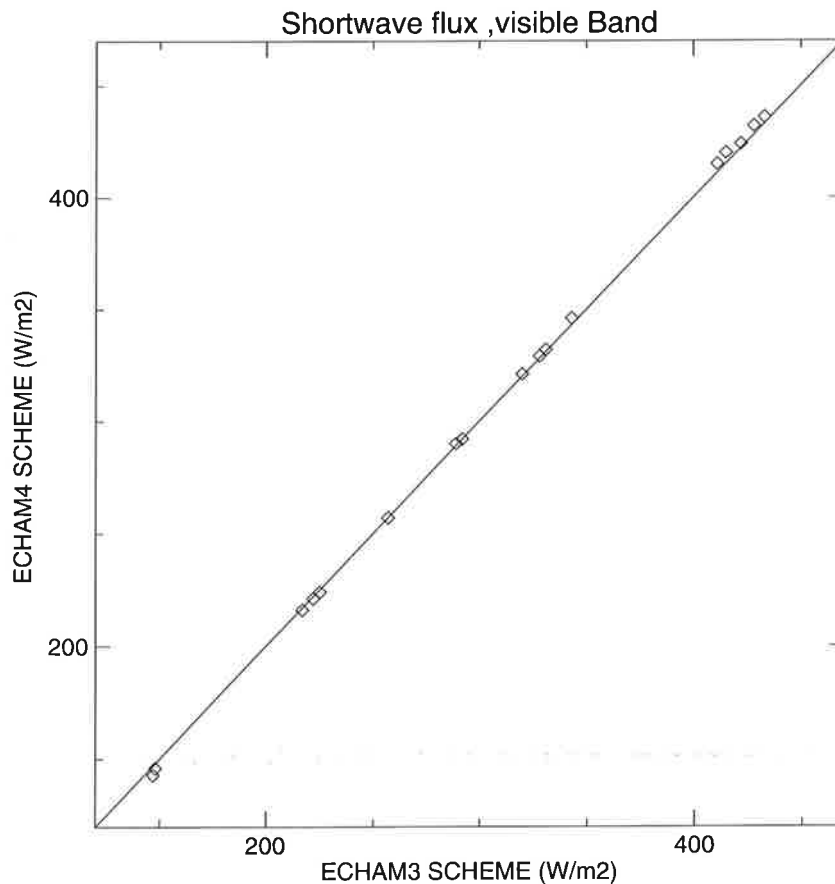


Figure 7: Incoming shortwave flux at the surface in the visible part of the spectrum ($0.2 - 0.7 \mu\text{m}$) calculated by the ECHAM3 and ECHAM4 radiation schemes in stand-alone mode for the clear-sky cases used in Figure 6.

More insight into the differences between the clear-sky computations of the ECHAM3 and ECHAM4 radiation schemes can be gained by a comparison of the individual spectral

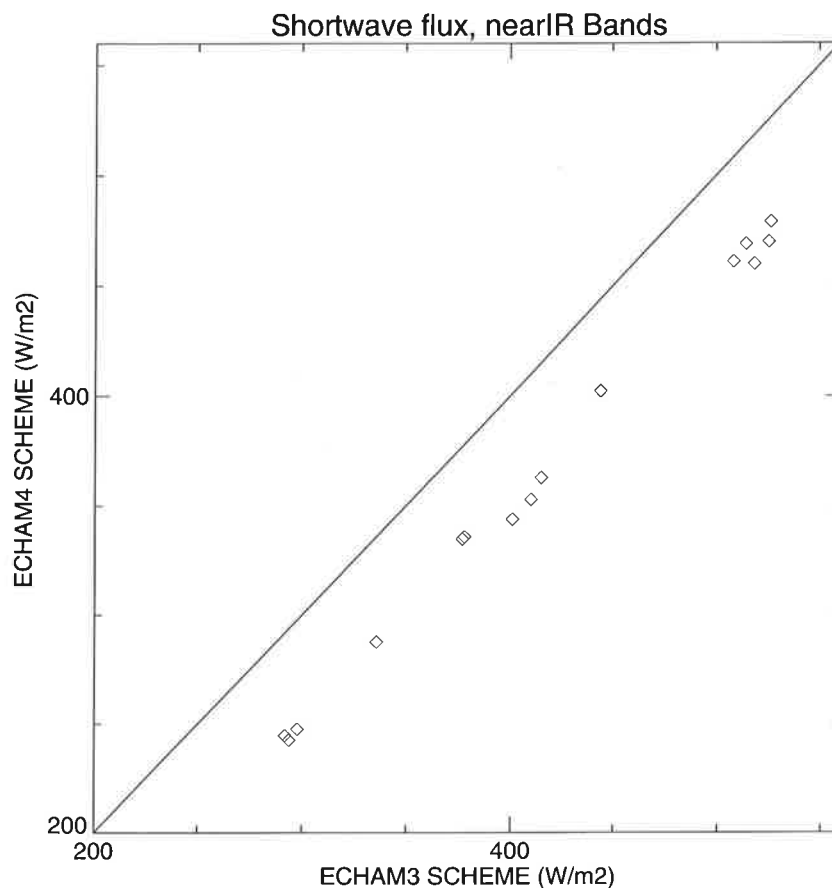


Figure 8: As Fig. 7, but for the near-infrared part of the spectrum (0.7 - 4.0 μm).

bands of the two models. The dimensions of the shortwave spectral intervals are given in Table 1. Although the number of bands is different in the two models, the separation between the visible band and the near-infrared bands is at the same wavelength (0.68 μm , cf. Table 1). This allows a direct comparison of the visible bands of the two schemes, while the near-infrared band of ECHAM4 has to be compared with the sum of three near-infrared bands of ECHAM3. This is done in Figs. 7 and 8 for the calculated clear-sky fluxes at the surface of the cases used before in Fig. 6. In the visible part, the calculated clear-sky fluxes of the two models are almost identical, the bias is virtually zero (Fig. 7). This also confirms that the effects of aerosols are identical in the two models. Since the models do not differ in the visible part, the 50 Wm^{-2} differences between the two schemes found above must be due to differences in the near-infrared bands. In fact large differences can be seen in Fig. 8, where the sum of the three near-infrared bands of ECHAM3 are compared with the corresponding ECHAM4 band. The ECHAM3 scheme calculates substantially higher near-infrared fluxes at the surface than ECHAM4, i.e. the near-infrared absorption of solar radiation in the ECHAM4 scheme is considerably larger than in ECHAM3. In the near-infrared, water vapour is the dominant absorber. The larger water vapour absorption of ECHAM4 is derived from a more recent spectroscopic dataset. The ECHAM3 radiation scheme was based on spectroscopic data of an early LOWTRAN version (LOWTRAN3, Selby and McClatchey, 1975), while the water vapor absorption

bands of the ECHAM4 scheme are derived from the AFGL spectroscopic dataset (Rothman et al., 1983). Models based on early LOWTRAN data have been shown to underestimate water vapour absorption compared to models based on AFGL data (Fouquart et al., 1991).

To summarize, the stand-alone validation indicates that the clear-sky shortwave radiative transfer is realistically captured in ECHAM4, which suggests that the 72 Wm^{-2} in Table 2 is a reasonable value for the solar absorption in the cloud-free atmosphere. Thus the increased clear-sky absorption is considered an important contributor to the improved atmospheric solar absorption and surface irradiances in ECHAM4.

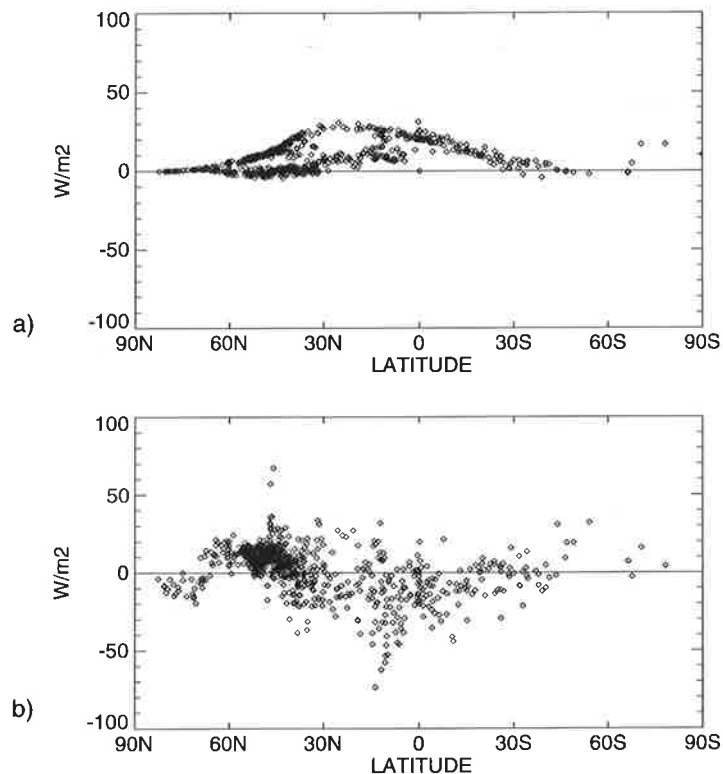


Figure 9:

a) Differences between ECHAM4 and ECHAM3-calculated shortwave absorption in the cloud-free atmosphere at the 720 GEBA sites as function of latitude.

b) Differences between ECHAM3-calculated shortwave atmospheric absorption, increased by the additional ECHAM4 clear-sky absorption of a), and observation-derived absorption at the 720 GEBA sites as function of latitude.

Differences between the atmospheric clear-sky absorption calculated by ECHAM4 and ECHAM3 are shown in Fig. 9a at the 720 GEBA sites used in Figs. 2 and 4. To illustrate the impact of the increased atmospheric clear-sky absorption, the extra ECHAM4 clear-sky absorption from Fig. 9a has been added to the ECHAM3 atmospheric all-sky absorption at each GEBA site and compared to the observation-derived values (Fig. 9b). Compared to the ECHAM3 atmospheric absorption in Fig. 2b, the additional ECHAM4 clear-sky absorption results in an improved simulation of atmospheric absorption and reduces the underestimated atmospheric absorption at low latitudes considerably. When assuming an accurate clear-sky simulation in Fig. 9b, the remaining bias has to be attributed to deficiencies in the calculated cloud absorption, which is discussed below.

5.2 Clouds

Two factors determine the interaction of clouds and radiation, namely the cloud radiative properties, and the spatial dimensions of the clouds, i.e. the cloud fraction.

In the ECHAM4 simulation, the global mean cloud fraction is with 0.60 substantially larger than in ECHAM3 with 0.52 at T42 and 0.50 at T106 resolution, respectively. Unlike ECHAM3, where a reduction of the cloud fraction with increasing resolution is found, the cloud fractions of the ECHAM4 T42 and T106 experiments are almost identical. The larger cloud fraction in ECHAM4 is in better agreement with observational estimates, which amount to 0.61 based on surface observations (Warren et al., 1986) and to 0.63 based on satellite observations (Rossow and Garder, 1993). The zonal simulation of cloud fraction over land, where most of the radiative flux measurements are available, is compared in Fig. 10 with the surface based climatology of Warren et al. (1986). ECHAM4 captures the zonal distribution of cloud fraction considerably better than ECHAM3. The improvement in ECHAM4 is evident at most latitudes. Especially for low latitudes, the agreement with the observations is excellent and the underestimated cloud amount found in ECHAM3 is no longer present in ECHAM4. The increased cloud amount in ECHAM4 is consistent with the reduced shortwave surface insolation at these latitudes. Since the shortwave balance at the TOA is very similar in ECHAM4 and ECHAM3 in the zonal mean, the impact of increased cloud fraction in ECHAM4 on the shortwave radiative fields is predominantly due to an increase in the cloud absorption rather than an increase in the reflection back to space.

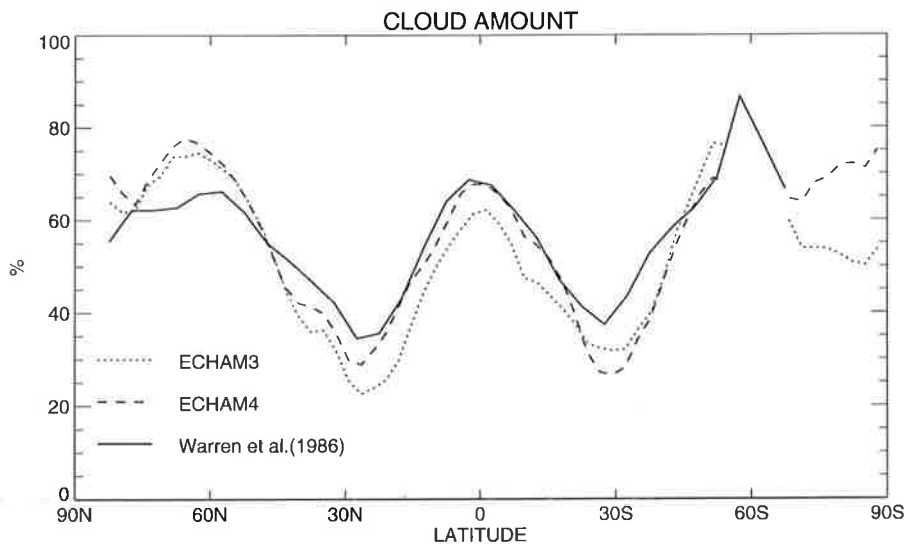


Figure 10: Zonal annual mean cloud amount over land: Simulations with ECHAM3 and ECHAM4 compared to the climatology of Warren et al. (1986). Units Percentage of cloud amount.

This can be quantified in the shortwave atmospheric cloud radiative forcing (CRF), i.e. the difference between the solar radiation absorbed in the all-sky and clear-sky atmosphere: The shortwave atmospheric CRF is enhanced from 8 Wm^{-2} in ECHAM3 to 18 Wm^{-2} in ECHAM4 on the global average (Table 2).

The increased cloud absorption is due to the following reasons:

i) As discussed above, ECHAM4 has an increased cloud fraction of 0.6 compared to the 0.5 in ECHAM3. This effect alone results in an additional absorption of 3 Wm^{-2} in the global mean.

ii) The ECHAM4 scheme resolves only two bands in the shortwave spectrum, while ECHAM3 has 4 bands (cf. Table 1). Slingo (1989) showed that a reduction of the number of shortwave bands below four can cause an artificial increase in the fraction of the spectrum available for absorption, resulting in a reduction of the single scattering albedo averaged over large bandwidths.

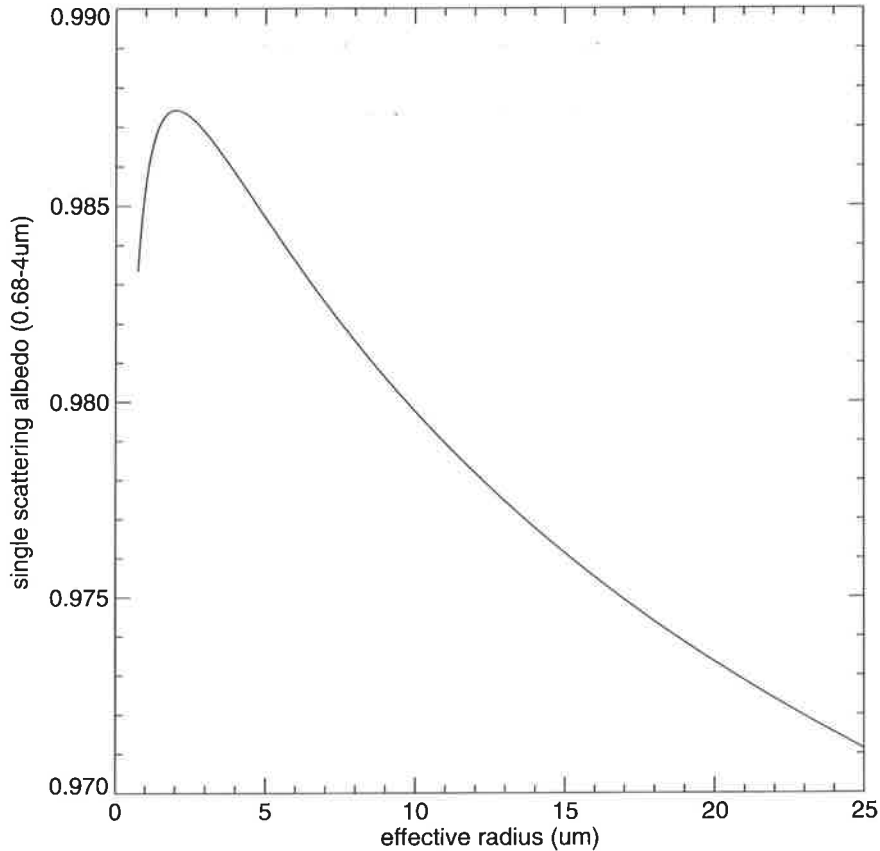


Figure 11: *Single scattering albedo as function of effective radius as parameterized in ECHAM4, based on Rockel et al. (1991).*

iii) ECHAM4 simulates substantially more low-level clouds than ECHAM3. Low-level clouds are characterized by high liquid water contents. Since the effective radii of cloud droplets are explicitly parameterized in terms of cloud water content in ECHAM4, the low level clouds with large droplet radii are particularly effective in the absorption of solar radiation. The cloud absorption is governed by the single-scattering albedo, which in ECHAM4 is determined as function of the effective radius. The dependence of the single scattering albedo on the effective radius for water clouds in ECHAM4 is shown in Fig. 11 for the near infrared band (in the visible band the single scattering albedo is constant at 0.9999). To get an estimate of typical values for the near-infrared single scattering albedo, a frequency distribution of effective radii in ECHAM4 has been diagnosed. The distribution shown is representative for warm clouds between 60°N and 60°S (at higher

latitudes the effective radii are generally close to the prescribed minimum effective radius of $4 \mu\text{m}$). The radii in the range of $5\text{-}10 \mu\text{m}$ over large parts of the globe suggest near-infrared single scattering albedos between 0.980 and 0.985 with a most frequent radius of $7\text{-}8 \mu\text{m}$ corresponding to a single scattering albedo near 0.982. The single scattering albedo in ECHAM3 for the three near-infrared bands is held constant at 0.999985 ($0.685\text{ - }0.891 \mu\text{m}$), 0.9996 ($0.891\text{ - }1.273 \mu\text{m}$) and 0.825 ($1.273\text{ - }3.580 \mu\text{m}$). Thus, the near-infrared single scattering albedo of ECHAM3 is higher than in ECHAM4 in the energy-important bands adjacent to the visible spectral range.

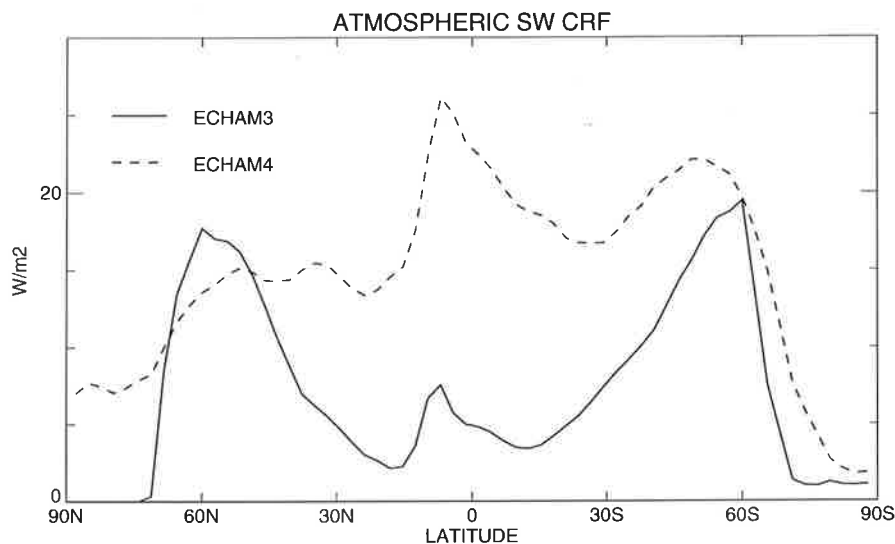


Figure 12: *shortwave cloud radiative forcing (SW CRF) in the atmosphere calculated with ECHAM3 and ECHAM4 (zonal annual mean), defined as the difference between the TOA and surface CRF, and representing the absorption of clouds in the atmosphere. Units Wm^{-2} .*

Zonally, the annual atmospheric CRF of ECHAM3 and ECHAM4 is compared in Fig. 12. In ECHAM4, the cloud absorption is enhanced at most latitudes, with a maximum in the tropics. An exception are the zones around 60°N/S where the ECHAM3 cloud absorption reaches or even exceeds the ECHAM4 values. The zonal distribution of atmospheric cloud radiative forcing is closely linked to the distribution of cloud water, which is shown in Fig. 13. The large cloud radiative forcing in ECHAM3 around 60°N/S is related to a maximum of cloud water in these areas. The zonal atmospheric CRF allows for a further interpretation of the differences between the model-calculated and observation-based atmospheric absorption in Figs. 2b (ECHAM3), 4b (ECHAM4) and 9b (ECHAM3 with ECHAM4 clear-sky fluxes). Figure 9b gave evidence, that the improved ECHAM4 clear-sky absorption alone cannot completely remove the underestimation of atmospheric absorption in low latitudes, but additional cloud absorption is needed. With the increased cloud absorption in ECHAM4, this underestimation of shortwave atmospheric absorption in low latitudes is eliminated and replaced by a slight tendency for an overestimation, in better agreement with the observations as noted before (Fig. 4b). For these latitudes, the Figures suggest that the increase in cloud absorption in ECHAM4 is beneficial, although quantitatively probably at the upper limit.

In higher latitudes, around 60°N/S , however, Figs. 2b, 4b and 9b suggest, that the cloud absorption is too high in both models. Note that the atmospheric absorption at

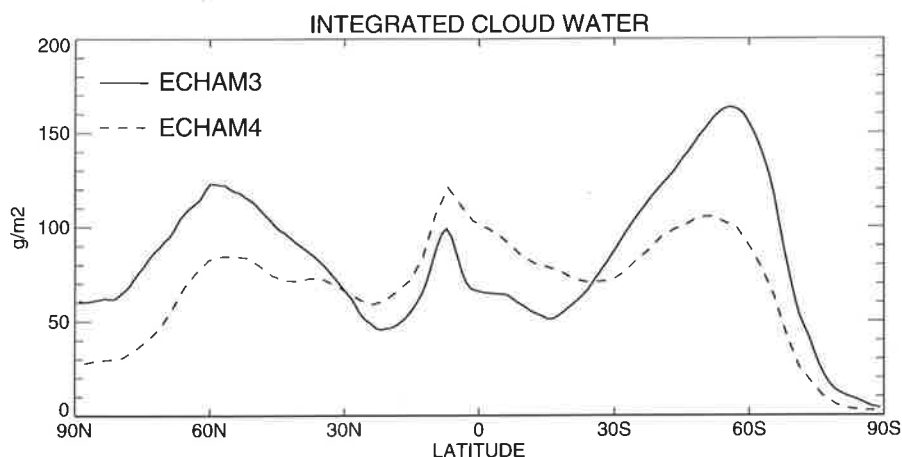


Figure 13: Vertically integrated cloud water calculated with ECHAM3 and ECHAM4 (Zonal annual mean). Units gm^{-2} .

these latitudes is similar in ECHAM3 and ECHAM4: the smaller clear-sky absorption in ECHAM3 is compensated by a larger cloud absorption around 60°N as can be inferred from Figs. 9a and 12.

The atmospheric CRF not only depends on the cloud optical properties, but also on the cloud amount as can be seen from the definition of the CRF. Therefore, the differences in the atmospheric CRF between the two models are not only caused by cloud optical properties, but are also influenced by differences in the cloud amount. To eliminate the effect of cloud amount and isolate the differences in cloud absorption due to changes in cloud optical properties between ECHAM3 and ECHAM4, the ratio R of cloud radiative forcing at the surface to the cloud radiative forcing at the TOA can be used. R has been introduced in the study of Cess et al. (1995), and observational evidence was presented therein, that R is close to 1.5 rather than around 1.1 found typically in GCMs, i.e. the shortwave radiation absorbed within clouds is suggested to be substantially higher than previously assumed. R has been increased from 1.16 in ECHAM3 to 1.35 in ECHAM4 in the global mean, as can be inferred from the TOA and surface cloud radiative forcings in Table 2. The zonal annual distribution of R is shown in Fig. 14 for the two models. It resembles the atmospheric cloud radiative forcing in many aspects: the differences between the two models are substantial at most latitudes except the zones around 60°N/S . However, with the elimination of the effects of cloud amount, the relative difference between the two models are reduced at low latitudes, where substantial differences in cloud amount exist (cf. Fig. 10). Similarly, the equatorial peak value of atmospheric CRF in the Innertropical convergence zone in both models due to the associated large cloud amounts is no longer seen in the zonal mean R .

The above comparisons with observational data indicate that both all-sky and clear-sky shortwave fluxes, as well as cloud amount, are reasonably captured in ECHAM4 over large parts of the globe. This suggests that, globally, the increased ECHAM4 cloud absorption as a residual is consistent with the observations and indicates that the R value of 1.35 in ECHAM4 may be more appropriate than the 1.16 in ECHAM3. This is in line with the studies of Cess et al. (1995) and Ramanathan et al. (1995). However, a further increase

of R up to 1.5 would definitely lead to a too small surface insolation of ECHAM4 at the GEBA sites, if not the clear-sky absorption or cloud amount would be reduced at the same time (for which there is no evidence from the above validations). Note that ECHAM4 may not provide a physical explanation for the increased cloud absorption, which is thought to be partly an artefact due to the low spectral resolution of the radiation scheme as outlined above. Nevertheless, it is of interest to see whether the increase in the absorption of solar radiation by clouds is consistent with the available observations.

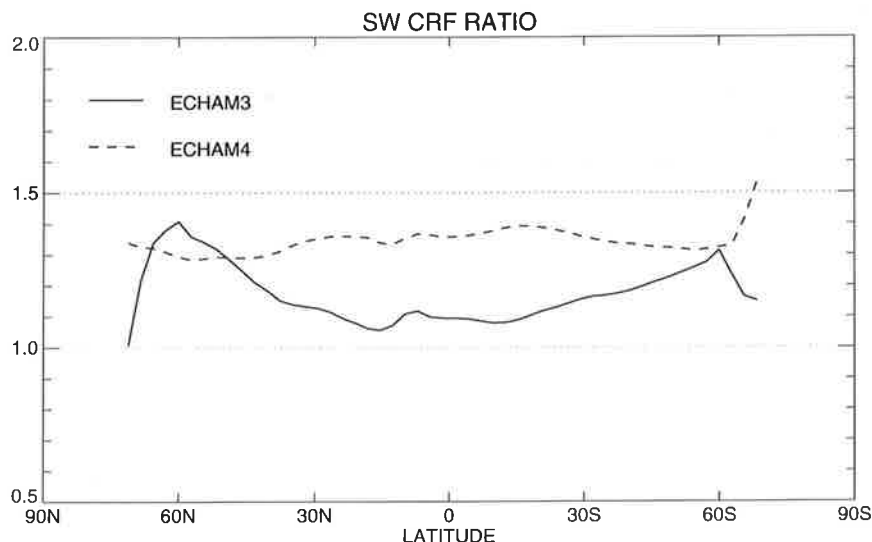


Figure 14: *Ratio of shortwave cloud radiative forcing at the surface to that at the top-of-atmosphere calculated with ECHAM3 and ECHAM4 (zonal annual mean).*

Zonally, at lower latitudes, the good performance of ECHAM4 implies that the R values of 1.35 - 1.4 in ECHAM4 are more realistic than the values near 1.1 in ECHAM3 (cf. Fig. 14). Again, a further increase of R beyond 1.4 at these latitudes may eventually result in a too high atmospheric absorption, considering that the atmospheric absorption calculated with ECHAM4 shows a slight tendency of overestimation rather than underestimation in Fig. 4b. Further, some of the differences between GCM-calculated and observed atmospheric absorption may be due to the presence of large loadings of aerosols related to biomass burning near the observation sites in equatorial areas, which are not taken into account in the GCM calculations (cf. Li et al., 1995). Konzelmann et al. (1996) suggest that black carbon aerosols can have a significant impact on the incoming shortwave radiation at GEBA sites in Equatorial Africa. No quantitative estimate of potential effects of such strongly absorbing aerosols are available so far due to the large uncertainty in the available aerosol data. At certain locations it cannot be excluded that aerosol from biomass burning rather than cloud absorption are the cause of the higher observed than calculated atmospheric absorption. This is suspected, however, only for a limited number of GEBA sites.

At higher latitudes, around 60°N/S , the above comparisons with observations give no evidence that R should be increased. Rather, only a lower value for R than the value near 1.3 presently found in both ECHAM3 and ECHAM4 around 60°N/S would reduce the discrepancies in Figs. 2b, 4b, 9b.

Thus, for lower latitudes, this analysis qualitatively supports a higher cloud absorption as suggested by Cess et al. (1995) and Ramanathan et al. (1995), but for higher latitudes, rather suggests a smaller value for R close to 1. Our results are consistent with the study of Li et al. (1995), who also found evidence for a zonal dependence of R with high values in low latitudes, but low values near 1 at high latitudes. Cess et al. (1995) suggested a uniformly high R of 1.5, while the R value of Ramanathan et al. (1995) has been derived in the tropics (western Pacific).

To summarize, the present study indicates that the enhanced cloud absorption in ECHAM4 is consistent with observations over large parts of the globe, but also underlines the importance of the clear-sky absorption in the explanation of the larger atmospheric absorption. A necessity to increase cloud absorption in GCMs is documented here for the low latitudes, but not so for higher latitudes.

6 Longwave radiation

The longwave balance at the earth's surface consists of the upward thermal emission from the surface and the downwelling atmospheric emission absorbed by the surface (incoming longwave radiation). While the modelling of the thermal emission of the surface is straightforward according to the Stefan-Boltzmann law, the incoming longwave flux has to be determined by comprehensive radiative transfer calculations which take into account the complex radiative characteristics of the atmosphere.

The global mean incoming longwave radiation calculated with different GCMs largely varies, as can be inferred from Fig. 15. The values shown vary within a range exceeding 30 Wm^{-2} . ECHAM4 exhibits a significantly higher global mean incoming longwave flux compared to ECHAM3 and other GCMs. Wild et al. (1995b) presented evidence that the incoming longwave radiation at the surface in ECHAM3 and other GCMs is underestimated by at least 10 Wm^{-2} . This has been confirmed in a recent study by Garratt and Prata (1996).

Wild et al. (1995b) identified the clear-sky performance of the radiation scheme as a major source for the underestimation. Using a stand-alone version of the radiation scheme they showed that the ECHAM3 radiation scheme calculates a too small longwave downward flux on the order of 10 Wm^{-2} under clear-sky conditions.

The longwave part of the ECHAM4 radiation scheme is based on the radiation code of the ECMWF Cycle 43 model (Morcrette, 1991). The original ECMWF scheme includes the water vapour continuum formulation of Roberts et al. (1976). This parameterization was modified at the Max-Planck Institute to include temperature-weighted band averages of e-type continuum and a band dependent ratio of (p-e)-type to e-type continuum absorption following Ma and Tipping (1992) (Giorgetta and Wild, 1995). These modifications result in an increase of the incoming longwave radiation of 10 Wm^{-2} compared to the original Morcrette scheme, which brings the ECHAM4 scheme in good agreement with observations in stand-alone calculations (Giorgetta and Wild, 1995).

The clear-sky performance of the ECHAM3 and ECHAM4 longwave radiation schemes is assessed in the following. Fig. 16 compares incoming longwave fluxes calculated with the ECHAM3 and ECHAM4 radiation schemes with in-situ observations. These calculations

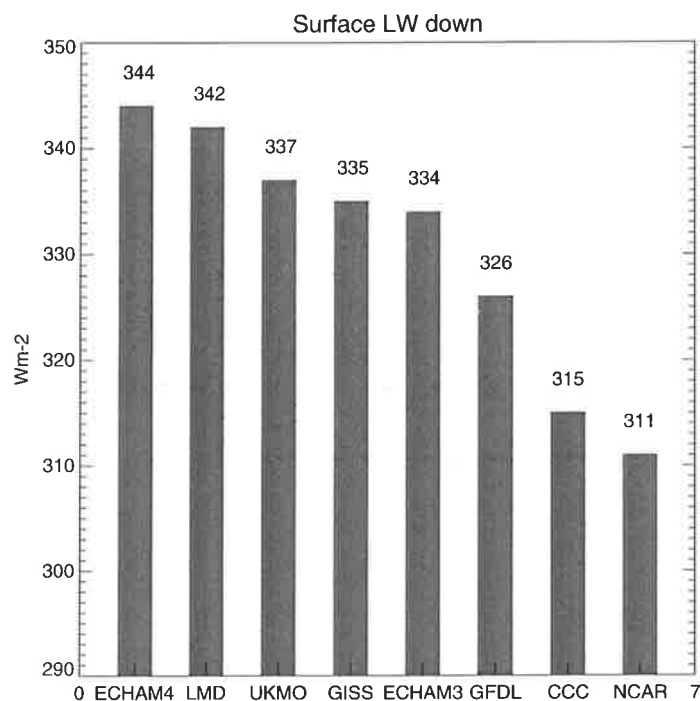


Figure 15: Global mean incoming longwave radiation at the surface calculated with ECHAM3, ECHAM4 and a number of other GCMs. NCAR, GFDL, GISS values from Gutowski et al. (1991), CCC value from Boer (1993), LMD value from J. Polcher (pers. communication, based on model version LMD6). UKMO value from H. Cattle (pers. communication). Units Wm^{-2} .

were again performed in stand-alone mode, with prescribed atmospheric profiles of humidity and temperature from radiosondes. The calculations were undertaken for a number of clear-sky conditions at midnight using observational data from the Swiss aerological station at Payerne. Fig. 16 shows that the ECHAM4 radiation scheme (including the modifications in the water vapour continuum) calculates systematically higher incoming longwave fluxes than the ECHAM3 scheme, in good agreement with observations. The average over the cases shown in Fig. 16 is 269.5 Wm^{-2} for the ECHAM3 scheme, 280.0 Wm^{-2} for the ECHAM4 scheme, and 278.4 Wm^{-2} observed. The bias of the ECHAM4 scheme (1.5 Wm^{-2}) is well within the measurement uncertainty, which is estimated to be $\pm 5 \text{ Wm}^{-2}$ for a single measurement. The 10.5 Wm^{-2} difference between the fluxes calculated with the ECHAM3 and ECHAM4 radiation scheme for clear-sky cases is similar to the differences found between the original ECMWF scheme and the modified scheme with higher emission of the water vapour continuum in (Giorgetta and Wild, 1995).

The 10.5 Wm^{-2} increase in the clear-sky flux of the ECHAM4 radiation scheme compared to the ECHAM3 scheme found in the stand-alone mode is reflected in the global mean values of the full three-dimensional GCM simulations: The global mean clear-sky incoming longwave radiation is 12 Wm^{-2} higher in ECHAM4 than in ECHAM3 according to Table 2. This Table also shows that the all-sky and clear-sky global mean values are increased by a very similar amount in ECHAM4. Thus, on the global scale, the increase in the incoming longwave radiation is mainly due to the increased downward emission of the cloud-free atmosphere, while the surface longwave cloud radiative forcing (impact of clouds

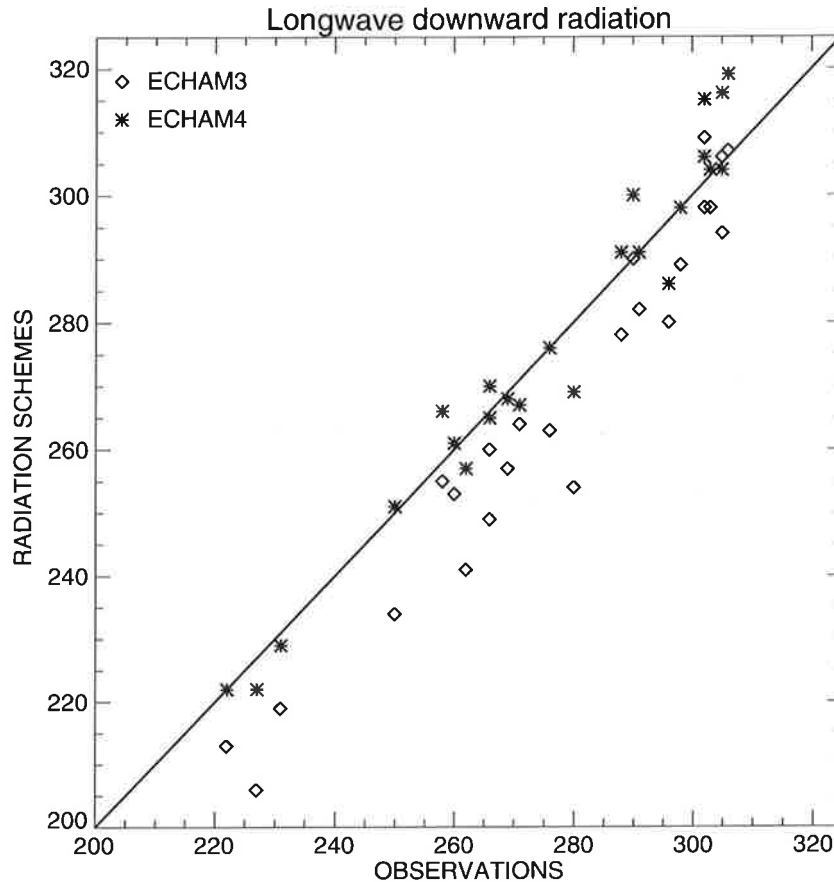


Figure 16: Incoming longwave radiation at the surface under clear-sky conditions at midnight: Stand-alone calculations with the ECHAM3 and ECHAM4 radiation schemes with prescribed atmospheric temperature and humidity profiles from radiosonde launches versus synchronous surface radiation measurements. Radiosonde data and radiation measurements from Payerne, Switzerland. Units Wm^{-2} .

on incoming longwave radiation) is similar in both model versions (cf. Table 2).

A number of stations monitoring the incoming longwave fluxes are available from the Global Energy Balance Archive. These sites have been used in Wild et al. (1995b) to document the systematic underestimation of the ECHAM3-calculated incoming longwave fluxes. The climatological annual cycles of incoming longwave radiation calculated with ECHAM4 at these sites are compared with ECHAM3 and the observations in Fig. 17. ECHAM4 shows at most sites an increased flux which reproduces the observed annual cycle more accurately than ECHAM3.

More long-term observations are urgently needed to improve the data basis for the assessment of the GCM simulated incoming longwave radiation. A major effort in this direction is currently undertaken with the establishment of the Baseline Surface Radiation Network (BSRN), which aims at the long-term monitoring of surface radiative fluxes at selected sites in different climatic regimes, equipped with best quality measurements (WCRP, 1991). Preliminary results of a comparison with a first series of data from a number of these stations indicate that zonally, the ECHAM4-calculated incoming longwave radiation shows a tendency for a slight overestimation in lower latitudes and underestimation in higher latitudes, which needs further analysis. Nevertheless, on the global average, the

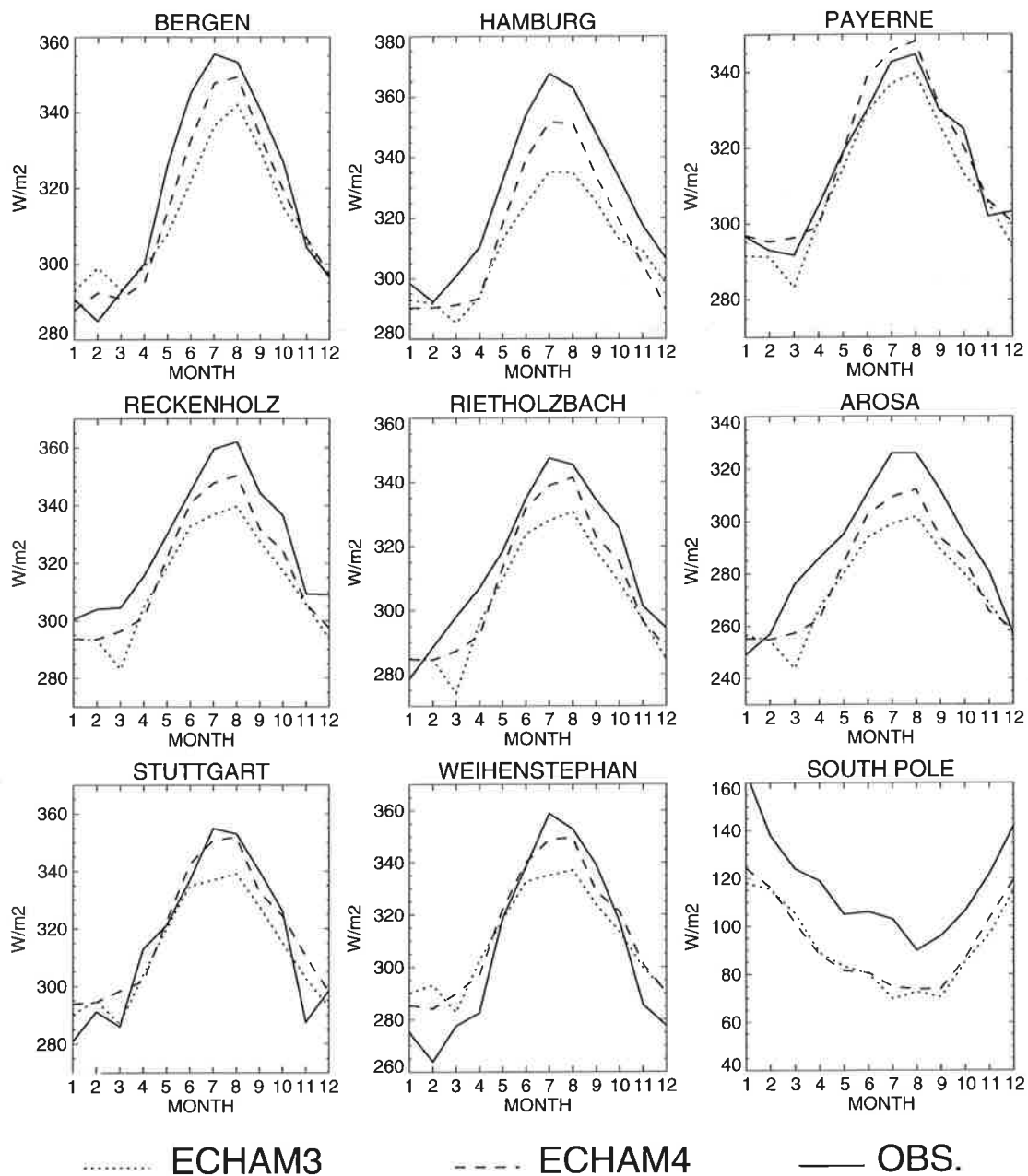


Figure 17: Annual cycles of model-calculated (ECHAM3, ECHAM4) and observed surface incoming longwave radiation at a number of stations from the Global Energy Balance Archive. Units W_m^{-2} .

sum of the available observational data and the stand-alone calculations with the radiation scheme suggest that the ECHAM4-calculated incoming longwave radiation of $344 W_m^{-2}$ is a realistic value. Note that the ECHAM4 model exhibits a significantly high global mean incoming longwave flux compared to other GCMs (Fig. 15). This further emphasizes a likely underestimation of the incoming longwave radiation typically found in other GCMs as evidenced by Wild et al. (1995b) and Garratt and Prata (1996).

The ECHAM4-simulated 344 Wm^{-2} of incoming longwave radiation also come close to the 350 Wm^{-2} estimated by Ohmura and Gilgen (1992), and to the 348 Wm^{-2} derived from satellite products by Rossow and Zhang (1995). The increased incoming longwave flux reduces the net longwave cooling at the surface from -63 Wm^{-2} in ECHAM3 to -53 Wm^{-2} in ECHAM4, as shown in Table 2 (The global mean surface temperature, and accordingly the upward longwave flux at the surface, changed insignificantly from ECHAM3 to ECHAM4).

With the net longwave cooling reduced by 10 Wm^{-2} , the reduction of shortwave surface absorption by 17 Wm^{-2} is partly compensated for, so that the available energy at the surface (surface net radiation) is only reduced by 7 Wm^{-2} in ECHAM4 in the global mean. Consequently, also the latent heat flux (the energy equivalent of the evaporation), which is driven by the surface net radiation, is not substantially reduced in ECHAM4. This ensures that the associated intensity of the global hydrological cycle does not become unrealistically weak (the evaporation is equal to the precipitation on a global average). The global mean precipitation in ECHAM4 amounts to 83 mm/month , while observed values range from 80 to 100 mm/months (Jaeger, 1976; Legates and Willmott, 1990; Spencer, 1993). Reducing only the surface shortwave absorption in GCMs (by enhancing the atmospheric clear-sky or cloud absorption as discussed in Section 5), on the other hand, may lead to a too small surface net radiation and accordingly, to a too weak global hydrological cycle.

An indirect indication for a higher incoming longwave radiation than previously assumed can therefore also be gained from the evidence for a reduced surface shortwave absorption and estimates of the global precipitation.

Thus, the global mean surface net radiation in ECHAM4 is with 95 Wm^{-2} not substantially different from other GCMs despite the reduced surface shortwave absorption (cf. compilation of surface net radiation values of several GCMs in Wild et al. (1995b)). However, while the surface net radiation in ECHAM3 and other models is only realistic due to an error cancellation between an overestimated surface insolation and underestimated incoming longwave radiation as evidenced in Wild et al. (1995b), these compensational errors are minimized in ECHAM4.

7 Conclusions

The surface and atmospheric radiation budgets simulated with ECHAM4 show substantially different values compared to earlier versions of the same model and other GCMs. This study supports these revised budgets using a comprehensive set of directly measured radiative fluxes.

The shortwave surface absorption in ECHAM4 is strongly reduced to 147 Wm^{-2} , due to a higher atmospheric absorption of 90 Wm^{-2} . A comparison with collocated measurements at the surface and from satellites at more than 700 sites supports these modifications. The 17 Wm^{-2} enhancement in the ECHAM4 atmospheric absorption compared to ECHAM3 is due to both increased atmospheric clear-sky and cloud absorption of similar magnitudes (9 Wm^{-2}). The increased atmospheric clear-sky absorption is consistent with observations: A stand-alone comparison of the ECHAM4 and ECHAM3 radiation schemes with in situ

measurements for clear-sky conditions showed a substantially reduced surface insolation calculated with the ECHAM4 scheme in good agreement with observations, while the ECHAM3 scheme produced systematic overestimation. The reduced surface insolation in ECHAM4 is due to an enhanced water vapour absorption in the near infrared band.

The present work presented evidence that both clear-sky and all-sky atmospheric absorptions are well captured in ECHAM4. This implies that the enhanced cloud absorption in ECHAM4 is not inconsistent with the observations over large parts of the globe. The present study thus does not contradict other studies suggesting a higher cloud absorption on the global scale, but at the same time points to the importance of the atmospheric clear-sky absorption for the explanation of existing differences between observed and GCM-calculated atmospheric absorption.

Zonally, observational evidence for a necessity to increase cloud absorption in GCMs is found in the low latitudes, but not so in higher latitudes: the comparisons favour a TOA-to-surface cloud radiative forcing ratio R of 1.3 - 1.4 in the tropics but closer to 1 in the extratropics.

Compared to ECHAM3, the net longwave cooling at the surface is reduced in ECHAM4, due to a 10 Wm^{-2} increase in incoming longwave radiation. This increase is due to an enhanced clear-sky atmospheric emission of the ECHAM4 radiation scheme with a modified water vapor continuum parameterization. The enhanced clear-sky incoming longwave flux is in good agreement with surface observations in stand-alone mode and no longer shows the systematic underestimation found in other radiation schemes. The available surface observations further support the larger incoming longwave flux in ECHAM4, which at 344 Wm^{-2} is substantially higher than in many other GCMs. In line with observations, the reduced surface shortwave absorption is compensated for by an increased incoming longwave flux, which allows to maintain the level of available energy at the surface required for a realistic intensity of the hydrological cycle. The problem of the error balance between overestimated surface insolation and underestimated incoming longwave radiation found in several GCMs (Wild et al., 1995b), which results in a superficially realistic surface net radiation on a global average, is largely reduced in ECHAM4. The global annual mean all-sky and clear-sky radiation budgets considered as most realistic based on the results of the present analysis are summarized in Fig. 18.

Acknowledgements:

The first author is indebted to Prof. L. Bengtsson for the possibility to frequently visit the MPI. Thanks to Drs. M. Beniston and M. Rotach for the careful review of the manuscript. The Swiss Scientific Computing Center CSCS generously provided computer resources, which allowed global climate simulations of unprecedented high resolution. The present work was financed through the Swiss National Science Foundation Grants National Research Program 31, Climate Change and Natural Hazards (Grant Nr. 4031-033250), Priority Program Environment (SPP, Grant Nr. 5001-35179), and ETH Grant Nr. 020-043-95.

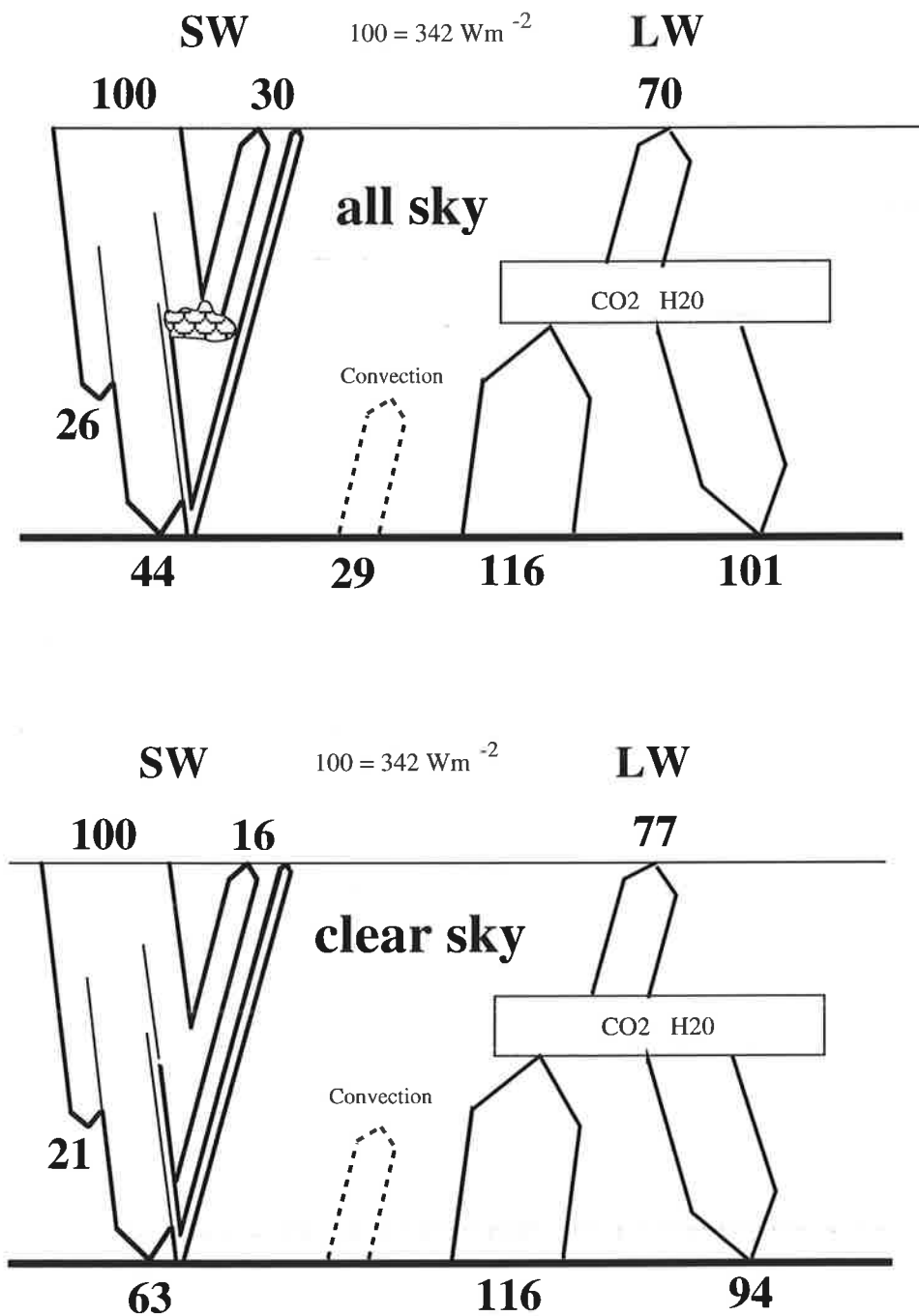


Figure 18: Global mean values of the earth's radiation budget considered as most realistic in the present analysis for climatological mean (all sky) and cloud free (clear sky) conditions. Units percentage of solar irradiance at the top-of-atmosphere.

References

- Barkstrom, B., 1984: The Earth Radiation Budget Experiment (ERBE). *Bull. Amer. Meteor. Soc.* **65**, 1170–1185.
- Barkstrom, B., E. Harrison, and R. Lee III, 1990: Earth Radiation Budget Experiment. *EOS* **71**, 297–305.
- Boer, G. J., 1993: Climate change and the regulation of the surface moisture and energy budgets. *Climate Dynamics* **8**, 225–239.
- Cess, R. D., M. Zhang, P. Minnis, L. Corsetti, E. Dutton, B. Forgan, D. Garber, W. Gates, J. Hack, E. Harrison, X. Jing, J. T. Kiehl, C. Long, J.-J. Mockett, G. Potter, V. Ramanathan, B. Subasilar, C. Whitlock, D. Young, and Y. Zhou, 1995: Absorption of solar radiation by clouds: observations versus models. *Science* **267**, 496–499.
- Chen, C.-T. and E. Roeckner, 1996: Validation of the earth radiation budget as simulated by the Max Planck Institute for Meteorology general circulation model ECHAM4 using satellite observations of the Earth Radiation Budget Experiment (ERBE). *J. Geophys. Res.* **101**, 4269–4287.
- Chen, C.-T., E. Roeckner, and B. Soden, 1996: A comparison of satellite observations and model simulations of column integrated moisture and upper tropospheric humidities. *J. Climate* (*in press*).
- Claussen, M., U. Lohmann, E. Roeckner, and U. Schulzweida, 1994: *A global data set of land-surface parameters*. Max Planck Institute for Meteorology Report No. 135. MPI for Meteorology, Bundesstrasse 55, D-20146 Hamburg.
- Dümenil, L. and E. Todini, 1992: A rainfall runoff scheme for use in the Hamburg Climate model. In J. O’Kane (Ed.), *advances in numerical hydrology. A tribute of James Dooge*, European Geophysical Society Series on Hydrological Sciences 1. Elsevier Science Publishers B.V.
- Fouquart, Y. and B. Bonnel, 1980: Computations of solar heating of the earth’s atmosphere: a new parameterization. *Beitr. Phys. Atmos.* **53**, 35–62.
- Fouquart, Y., B. Bonnel, and V. Ramaswamy, 1991: Intercomparing shortwave radiation codes for climate studies. *J. Geophys. Res.* **96**, 8929–8953.
- Garratt, J. R., 1994: Incoming shortwave fluxes at the surface - a comparison of GCM results with observations. *J. Climate* **7**, 72–80.
- Garratt, J. R. and A. Prata, 1996: Downwelling longwave fluxes at continental surfaces - a comparison of observations with GCM simulations and implications for the global land-surface radiation budget. *J. Climate* (*in press*).
- Gates, W. L., 1992: AMIP: The atmospheric model intercomparison project. *Bull. Amer. Meteor. Soc.* **73**, 1962–1970.
- Geleyn, J. F. and H. J. Preuss, 1983: A new data set of satellite-derived surface albedo values for operational use at ECMWF. *Arch. Meteor. Geophys. Bioclim. Ser. A.* **32**, 353–359.
- Gilgen, H., M. Wild, T. Konzelmann, and A. Ohmura, 1996: Global climatology of shortwave incoming radiation at the surface using the Global Energy Balance Archive

- (GEBA). *J. Climate* (submitted).
- Giorgetta, M. and M. Wild, 1995: *The water vapor continuum and its representation in ECHAM4*. Max Planck Institute for Meteorology Report No. 162. MPI for Meteorology, Bundesstrasse 55, D-20146 Hamburg.
- Gutowski, W. J., D. S. Gutzler, and W. C. Wang, 1991: Surface energy balances of three general circulation models: implications for simulating regional climate change. *J. Climate* **4**, 121–134.
- Hense, A., M. Kerschgens, and E. Raschke, 1982: An economical method for computing radiative transfer in circulation models. *Quart. J. Roy. Meteor. Soc.* **108**, 231–252.
- Jaeger, L., 1976: *Monatskarten des Niederschlags fuer die ganze Erde*. Ber. d. Dt. Wetterdienstes 139. Offenbach: Dt. Wetterdienst.
- Kerschgens, M. U., E. Pilz, and E. Raschke, 1978: A modified two stream approximation for computations of the solar radiation budget in a cloudy atmosphere. *Tellus* **30**, 429–435.
- Kiehl, J., J. Hack, M. Zhang, and R. Cess, 1995: Sensitivity of a GCM Climate to enhanced shortwave cloud absorption. *J. Climate* **8**, 2200–2212.
- Konzelmann, T., D. Cahoon, and C. Whitlock, 1996: Impact of biomass burning in Equatorial Africa on the downward surface shortwave irradiance: observations and calculations. *J. Geophys. Res.* (in press).
- Legates, D. R. and C. J. Willmott, 1990: Mean seasonal and spatial variability in gage-corrected global precipitation. *Int. J. Climatology* **10**, 111–127.
- Li, Z. and H. Barker, 1994: Solar energy disposition: Intercomparison between satellite estimation, GCM simulation, and surface observations. In *WCRP Report - IAMAS International Workshop on Clouds-Radiation Interactions and their Parameterization in Climate Models*. Camp Springs, MD, Oct. 1993.
- Li, Z., H. Barker, and L. Moreau, 1995: The variable effect of clouds on atmospheric absorption of solar radiation. *Nature* **376**, 486–490.
- Li, Z. and H. G. Leighton, 1993: Global climatologies of solar radiation budgets at the surface and in the atmosphere from 5 years of ERBE data. *J. Geophys. Res.* **98**, 4919–4930.
- Li, Z., C. H. Whitlock, and T. P. Charlock, 1995: Assessment of the global monthly mean surface insolation estimated from satellite measurements using Global Energy Balance Archive data. *J. Climate* **8**, 315–328.
- Ma, Q. and R. Tipping, 1992: A far wing line shape theory and its application to the foreign-broadened water continuum absorption. *J. Chem. Phys.* **97**, 818–828.
- Morcrette, J., 1991: Radiation and cloud radiative properties in the european centre for medium range weather forecasts forecasting system. *J. Geophys. Res.* **96**, 9121–9132.
- Morcrette, J., L. Smith, and Y. Fouquart, 1986: Pressure and temperature dependence of the absorption in longwave radiation parameterizations. *Beitr. Phys. Atmos.* **59**, 455–469.

- Ohmura, A. and H. Gilgen, 1992: Global Energy Balance Archive (GEBA, WCP-water A7) and new aspects of the global radiation distribution on the earth's surface. In Keevallik and Kaerner (Eds.), *IRS '92, Current problems in atmospheric radiation*, pp. 271–274. DEEPAK Publishing.
- Ohmura, A., H. Gilgen, and M. Wild, 1989: *Global Energy Balance Archive GEBA, World Climate Program - Water Project A7, Report 1: Introduction*. Zürcher Geografische Schriften No. 34. Zürich: Verlag der Fachvereine.
- Ramanathan, V., B. Subasilar, G. Zhang, W. Conant, R. Cess, J. Kiehl, H. Grassl, and L. Shi, 1995: Warm pool heat budget and shortwave cloud forcing: a missing physics? *Science* **267**, 499–503.
- Randall, D. A., R. D. Cess, J. P. Blanchet, G. J. Boer, D. A. Dazlich, A. D. D. Genio, M. Deque, V. Dymnikov, V. Galin, S. J. Ghan, A. A. Lacis, H. L. Treut, Z. X. Li, X. Z. Liang, B. J. McAveney, V. P. Meleshko, J. F. B. Mitchell, J. J. Mcrette, G. L. Potter, L. Riskus, E. Roeckner, J. F. Royer, U. Schlese, D. A. Sheinin, J. Slingo, A. P. Sokolov, K. E. Taylor, W. M. Washington, R. T. Wetherald, I. Yagai, and M. H. Zhang, 1992: Intercomparison and interpretation of surface energy fluxes in atmospheric general circulation models. *J. Geophys. Res.* **97**, 3711–3722.
- Roberts, R., J. Selby, and L. Biberman, 1976: Infrared continuum absorption by atmospheric water vapor in the 8 - 12 μm window. *Appl. Opt.* **15**, 2085–2090.
- Rockel, B., E. Raschke, and B. Weyres, 1991: A parameterization of broad band radiative transfer properties of water, ice and mixed clouds. *Beitr. Phys. Atmos.* **64**, 1–12.
- Roeckner, E., 1995: Parameterization of cloud radiative properties in the ECHAM4 model. In *Proceedings of the WCRP workshop on "Cloud Microphysics Parameterizations in Global Atmospheric Circulation Models", May 23-25, 1995, Kananaskis, Alberta, Canada, WCRP-90, WMO/TD-No. 713*, pp. 105–116.
- Roeckner, E., K. Arpe, L. Bengtsson, S. Brinkop, L. Dümenil, M. Esch, E. Kirk, F. Lunkeit, M. Ponater, B. Rockel, R. Sausen, U. Schlese, S. Schubert, and M. Windelband, 1992: *Simulation of the present day climate with the ECHAM model: impact of model physics and resolution*. Max Planck Institute for Meteorology Report No. 93. MPI for Meteorology, Bundesstrasse 55, D-20146 Hamburg.
- Roeckner, E., K. Arpe, L. Bengtsson, M. Christoph, M. Claussen, L. Dümenil, M. Esch, M. Giorgetta, U. Schlese, and U. Schulzweida, 1996: *The Max Planck Institute for Meteorology fourth-generation atmospheric general circulation model ECHAM4: Model description and climatology*. Max-Planck Institute for Meteorology Report, in preparation.
- Roeckner, E., M. Rieland, and E. Keup, 1991: Modelling of cloud and radiation in the ECHAM model. In *ECMWF/WCRP Workshop on "clouds, radiative transfer and the hydrological cycle*, pp. 199–222. Reading.
- Rossow, W. and Y.-C. Zhang, 1995: Calculation of surface and top of atmosphere radiative fluxes from physical quantities based on ISCCP data sets. Part II: Validation and first results. *J. Geophys. Res.* **100 (D1)**, 1167 – 1197.
- Rossow, W. B. and L. C. Garder, 1993: Validation of ISCCP cloud detections. *J. Climate* **6**, 2370–2393.

- Rothman, L.S., R. Gamache, A. Barbe, A. Goldman, J. Gillis, L. Brown, R. Toth, J. Flaud, and C. Camy-Peyret, 1983: AFGL atmospheric absorption line parameters compilation: 1982 edition. *Appl. Opt.* **15**, 2247–2256.
- Selby, I. and R. McClatchey, 1975: Atmospheric transmittance from 0.25 - 28.5 μm , computer code LOWTRAN 3. Technical report.
- Shettle, E. and R. Fenn, 1976: Models of the atmospheric aerosols and their optical properties. Technical Report AGARD-CP-183, AGARD Conference Proceedings No. 183.
- Slingo, A., 1989: A GCM parameterization for the shortwave radiative properties of water clouds. *J. Atmos. Sci.* **46**, 1419–1427.
- Spencer, R., 1993: Global oceanic precipitation from MSU during 1979-1991 and comparisons to other climatologies. *J. Climate* **6**, 1301–1326.
- Stephens, G. L., 1978: Radiation profiles in extended water clouds: 2. parameterization schemes. *J. Atm. Sci.* **35**, 2123–2132.
- Warren, S. G., C. J. Hahn, J. London, R. M. Chervin, and R. L. Jenne, 1986: Global distribution of total cloud cover and cloud type amounts over land. Technical Report DOE / ER / 60085-H1, NCAR / TN-273+STR, NCAR.
- WCRP, 1991: Radiation and Climate, Second workshop of the baseline surface radiation network. Technical Report WCRP-64, Geneva.
- Wild, M., L. Dümenil, and J. Schulz, 1996: Regional climate simulation with a high resolution GCM: surface hydrology. *Climate Dynamics (in press)*.
- Wild, M., A. Ohmura, H. Gilgen, and E. Roeckner, 1995a: Regional climate simulation with a high resolution GCM: surface radiative fluxes. *Climate Dynamics* **11**, 469–486.
- Wild, M., A. Ohmura, H. Gilgen, and E. Roeckner, 1995b: Validation of GCM simulated radiative fluxes using surface observations. *J. Climate* **8**, 1309–1324.
- Zdunkowski, W. G., R. M. Welch, and G. Korb, 1980: An investigation of the structure of typical two stream methods for the calculation of solar fluxes and heating rates in clouds. *Beitr. Phys. Atm.* **53**, 147–166.